

Some Mobile VHF Measurements in an Urban Environment

C.J. Chilton
H.B. Janes
R.A. McLean
D. Smith



U.S. DEPARTMENT OF COMMERCE
Malcolm Baldrige, Secretary

Dale N. Hatfield, Acting Assistant Secretary
for Communications and Information

January 1981

TABLE OF CONTENTS

	PAGE
LIST OF FIGURES	iv
ABSTRACT	1
1. INTRODUCTION	1
2. EXPERIMENTAL MEASUREMENTS	5
3. THEORETICAL CONSIDERATIONS AND DATA ANALYSIS	14
3.1 Statistical Analysis of the June and July Data	14
3.2 Power Spectrum Analysis	15
3.3 Doppler Fading and Standing Waves	24
3.4 Statistical Analysis of the August Data	26
4. DISCUSSIONS AND RECOMMENDATIONS	33
5. REFERENCES	37
APPENDIX	39

·LIST OF FIGURES

Figure No.		Page
1.	Test location area showing Lookout Mountain TV Transmitter and routes taken by mobile measurement van.	3
2.	Mobile measurement VHF antenna mounted on van.	4
3.	Television Channel 2 (KWGN) spectrum measured at 10th and Ford Street in Golden, Colorado.	6
4.	Television Channel 4 (KOA) spectrum measured at 10th and Ford Street in Golden, Colorado.	7
5.	Television Channel 7 (KMGH) spectrum measured at 10th and Ford Street in Golden, Colorado	8
6.	Television Channel 9 (KBTv) spectrum measured at 10th and Ford Street in Golden, Colorado.	9
7.	Typical signal variation of KWGN at a mobile speed of 20 mph. Run 11 on 6/6/79, East at 20 mph, Channel 2 at 55.25 MHz (video) and 59.75 MHz (audio).	10
8.	Typical signal variation of KOA at a mobile speed of 20 mph. Run 13 on 6/6/79, East at 20 mph, Channel 4 at 67.25 MHz (video) and 71.74 MHz (audio).	11
9.	Typical signal variation of KMGH at a mobile speed of 20 mph. Run 17 on 6/6/79, East at 20 mph, Channel 7 at 175.25 MHz (video) and 179.75 MHz (audio).	12
10.	Typical signal variation of KBTv at a mobile speed of 20 mph. Run 15 on 6/6/79 going East at 20 mph on the 0.7 mile test course. Channel 9 (KBTv) at 187.24 MHz (video) and 191.74 MHz (audio).	13
11.	The relative frequency diagram which is an approximation to the probability density function for the data of Run 15.	16
12.	Cumulative probability distribution for the data of Run 15 plotted on Rayleigh paper.	17
13.	Cumulative probability distribution for the data of Run 15 plotted on Gaussian paper.	18
14.	Correlation coefficient between the audio and video signals for Run 15.	19
15.	Signal envelope for Runs 15 and 16 with Run 15 reversed and shifted 300 points.	20

16.	Correlation coefficients for Runs 15 and 16.	21
17.	Power spectra for Run number 15 for video and audio data at 20 mph.	22
18.	Power spectra for Run number 16 for video and audio data at 20 mph.	23
19.	Composite plot of West bound Channel 9 (KBTv) video data power spectrum at 10, 20, and 30 mph.	25
20.	14 August '79 data for segment number 1, Channel 9 (KBTv) at 187.24 MHz (Video).	27
21.	14 August '79 data for segment number 4, Channel 9 (KBTv) at 187.24 MHz (Video).	28
22.	14 August '79 data for segment number 5, Channel 9 (KBTv) at 187.24 MHz (Video).	29
23.	Power spectrum for segment number 1.	30
24.	Power spectrum for segment number 4.	31
25.	Power spectrum for segment number 5.	32
26.	Composite plot of CDF for segments 1, 4, 5, and 24 showing the deviation from a Rayleigh distribution that can occur in the urban environment.	34
27.	Standard deviation of the data segments on the 14 August 1979 6th Avenue, Valley Highway, I-70 loop.	35
28.	Mean value of the signal envelope for each data segment of 14 August 1979.	36

SOME MOBILE VHF MEAUREMENTS IN AN
URBAN ENVIRONMENT

C. J. Chilton, H. B. Janes^{*}, R. A. McLean, and D. Smith^{**}

This report presents the results of mobile measurements of VHF signals in the Denver, Colorado, urban environment. The signals monitored were those received from the TV transmissions of KBTB (Channel 9), KMGH (Channel 7), KOA (Channel 4), and KWGN (Channel 2) from transmitting antennas located on top of Lookout Mountain. The statistical analysis of the data implies that the signal fading mechanism does not always have Rayleigh probability density distribution, and could possibly be better described by an exponential Weibull distribution. In addition, a new analysis technique was developed to normalize the data by calculating a power density spectrum as a function of an inverse distance (wave number) which gives a means of comparing data taken at different times on different days and at different vehicle velocities in such a way as to make it possible to separate the position dependent effects from the time dependent properties.

Key words: mobile radio communication; statistical analysis; VHF;
VHF radio propagation

1. INTRODUCTION

It is well known that fluctuations in the received signal amplitude occur during mobile communication measurement. These variations are due to the motion of the mobile measuring van through the spatial standing wave pattern that results from the interaction of the direct and reflected waves (Jakes, 1974). In addition, there are also time variations due to other moving reflectors and atmospheric variability. As pointed out by Jakes (1974), "These observations seem to defy any attempt at a systematic interpretation or quantitative analysis." Nevertheless, several models based on multipath wave interference (Ossanna, 1964) and statistical communication theory (Clarke, 1968) have been used with considerable success to explain many of the features observed in mobile measurements of VHF and UHF signals. A radio signal transmitted to a moving vehicle in an urban environment exhibits large variations in both the amplitude and apparent frequency. When there is no line-of-sight (LOS) path to the receiver, the mode of propagation of the electromagnetic energy from the transmitter to the receiver is thus either by way of scattering, including reflection from the flat surface of buildings and man-made or natural obstacles, or by diffraction around such objects; and when the LOS signal is present there can be standing wave effects produced by the direct and

* H. B. Janes is with OAO Corporation, Lakewood, CO 80228

** C. J. Chilton, R. A. McLean and D. Smith are with the U.S. Department of Commerce National Telecommunications and Information Administration, Institute for Telecommunication Sciences, Boulder, CO 80303.

reflected waves. One could attempt to study this propagation phenomenon by separating the multipath wave structure into individual ray components and identifying the propagation mode on the basis of arrival angle, since the multipath signals arrive from unique directions, or on the basis of the propagation delay time relative to the line-of-sight signal. Since this "ray theoretical" technique is somewhat difficult to implement experimentally [although it has been recently used by Ikegami and Yoshida (private communication) to study mobile VHF multipath propagation structure at Kyoto University in Japan], a statistical theory is generally used since the signal envelope can be more directly measured. The statistical model used assumes that the field incident on the receiver antenna is composed of randomly phased plane waves of arbitrary azimuth angles. The statistical characteristics of the received signals are then deduced from a statistical propagation model; i.e., the probability density that determines if the signal envelope will be found within a narrow range around a given level and the cumulative distribution, the percent of time it lies above a given level are calculated.

In addition to the randomly phased waves, each plane wave component has a "Doppler shift," which is a function of the speed of the vehicle, the angle the wave propagation vector makes with mobile velocity vector, and the transmitter carrier frequency. One can then express the observed fluctuations as being due to the beating within the receiver of all the frequencies arising from the different Doppler shifts occurring for the direct incident and the reflected waves.

The primary purpose of this report is to present some recent measurements made using the TV transmitters located on top of Lookout Mountain near Golden, Colorado. The signals monitored were KBTv (189 MHz), KMGH (177 MHz), KOA (69 MHz), and KWGN (57 MHz). Mobile measurements of these signals were made at several vehicle speeds along 44th Avenue in Golden, Colorado, and along a 50-mile loop through Denver (Figure 1). The antenna used is a modified version of a miniature VHF directional antenna system originally designed to provide continuous coverage of the 30 to 200 MHz frequency range and is shown mounted on the measurement van in Figure 2. The receiver system is the Hewlett-Packard ARS-400 installed in a mobile van. A secondary purpose of this report is to describe a somewhat novel approach to analyzing data taken using a computerized mobile measuring system. This new approach involves calculating the spectral density of the signal envelope as a function of wave-number which has units of inverse distance rather than as a function of frequency. This technique allows the data to be viewed as a spatial variation rather than as a time variation, and thereby provides a possible means of identifying position dependent (stationary) effects in the data separable from those that

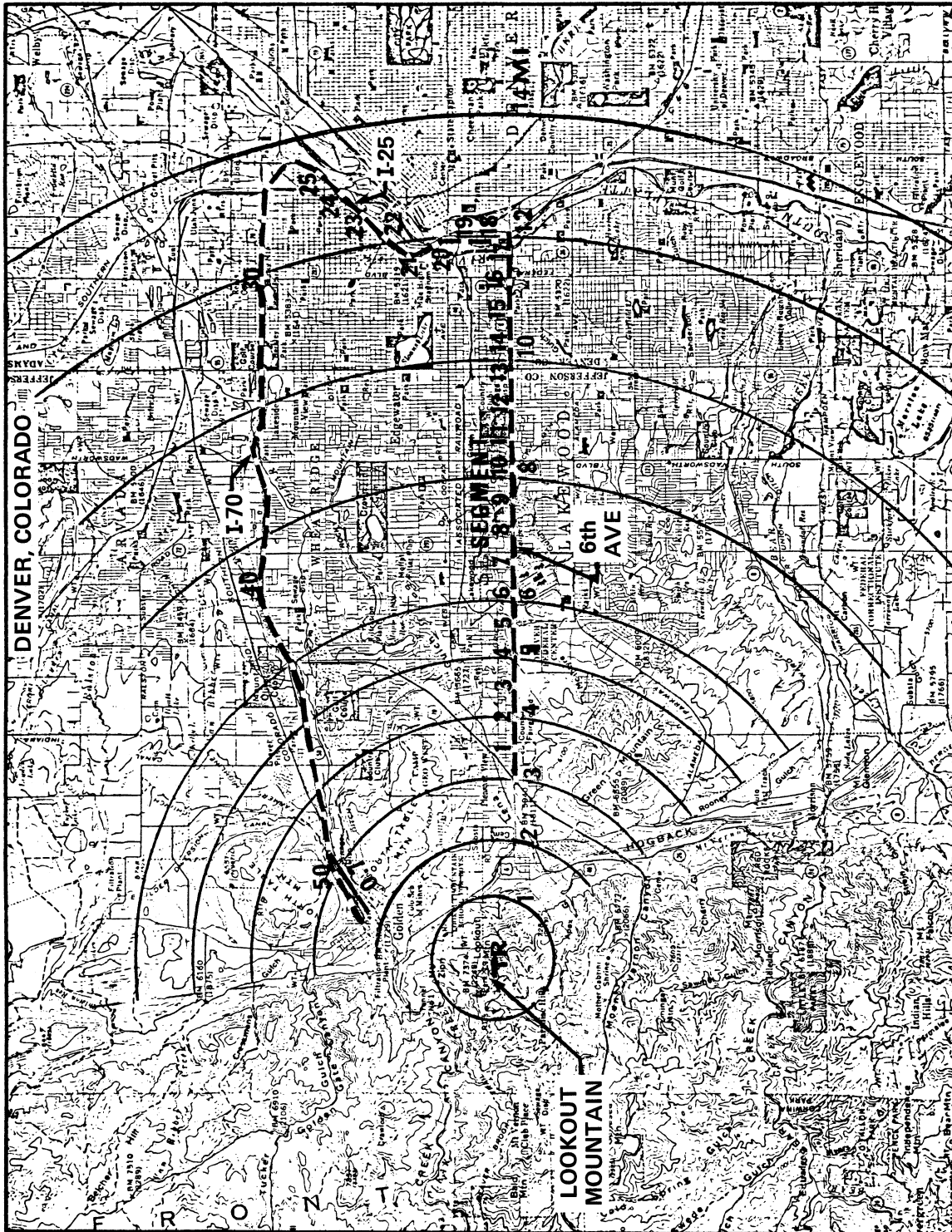


Figure 1. Test location area showing Lookout Mountain TV transmitter and routes taken by mobile measurement van.

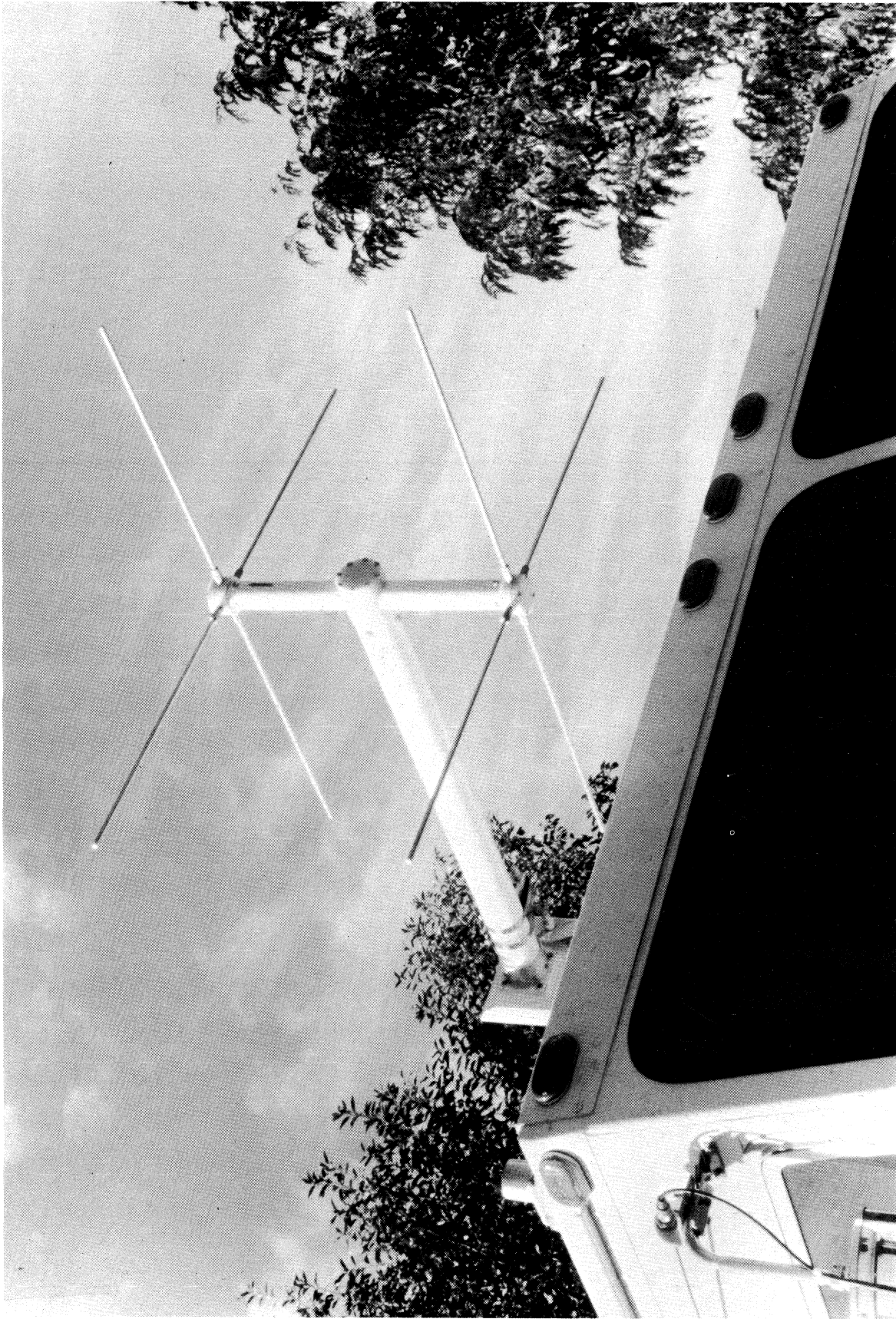


Figure 2. Mobile measurement VHF antenna mounted on van.

are time dependent (nonstationary), since the vehicle speed is "normalized" and only the distance traveled by the vehicle between measurements is used as the independent variable.

2. EXPERIMENTAL MEASUREMENTS

The measurements presented in this report were obtained over a test course of approximately 0.7 mi (1200 meters), which simulated the urban environment of large steel and concrete buildings. This 0.7 mi stretch of road is located between the second and third radial mile northeast from the transmitter on Lookout Mountain (solid line in Figure 1). Additional data were taken on an approximate 30 mi loop east from the transmitter on 6th Avenue to the Valley Highway, north on the Valley Highway to Interstate 70, and then west on I-70 back toward the transmitter near Golden, Colorado (dashed in Figure 1). The data taken on the 0.7 mi test course were obtained at vehicle speeds from 0 to 40 mph.

The spectral distribution of the four TV transmitter signals monitored are shown in Figures 3 through 6. The relative amplitude power of the audio and video carriers are given in dB relative to a milliwatt (dBm), and the frequency scale is in megahertz (MHz) along the assigned bandwidth. The receiver bandwidth was 100 kHz. These measurements were made at the beginning of the 0.7 mi test course on 6 June 1979.

All the measurements presented here were made using a radio frequency (rf) measurement system for automatic signal monitoring and analysis in the 100 kHz to 18 GHz frequency range. The instrument is a computer controlled receiver which can filter and detect rf signals, convert these signals to digital data, and process and output these data to display, hard copy, and tape storage devices. Examples of the typical received signal variations (audio and video for each of the four TV transmitters) measured at a mobile speed of 20 mph are shown in Figures 7 through 10. All of the data taken were digitally recorded on magnetic tape for further processing at a later time. The measurements were conducted on 6 June, 24 July, and 14 August, 1979. The 6 June 1979 measurements were all made at a mobile speed of 20 mph and a receiver bandwidth of 100 kHz. The 24 July 1979 measurements were made at mobile speeds of 10, 20, 30, and 40 mph, and a receiver bandwidth of 300 kHz. Both the 6 June and the 24 July measurements were conducted on the 0.7 mi test course shown in Figure 1. The 14 August measurements were carried out on the 30 mi 6th Avenue-Valley Highway - Interstate 70 loop at a mobile speed of 40 mph and a receiver bandwidth of 10 kHz.

CHANNEL 2 (10th & FORD, GOLDEN, COLO.)

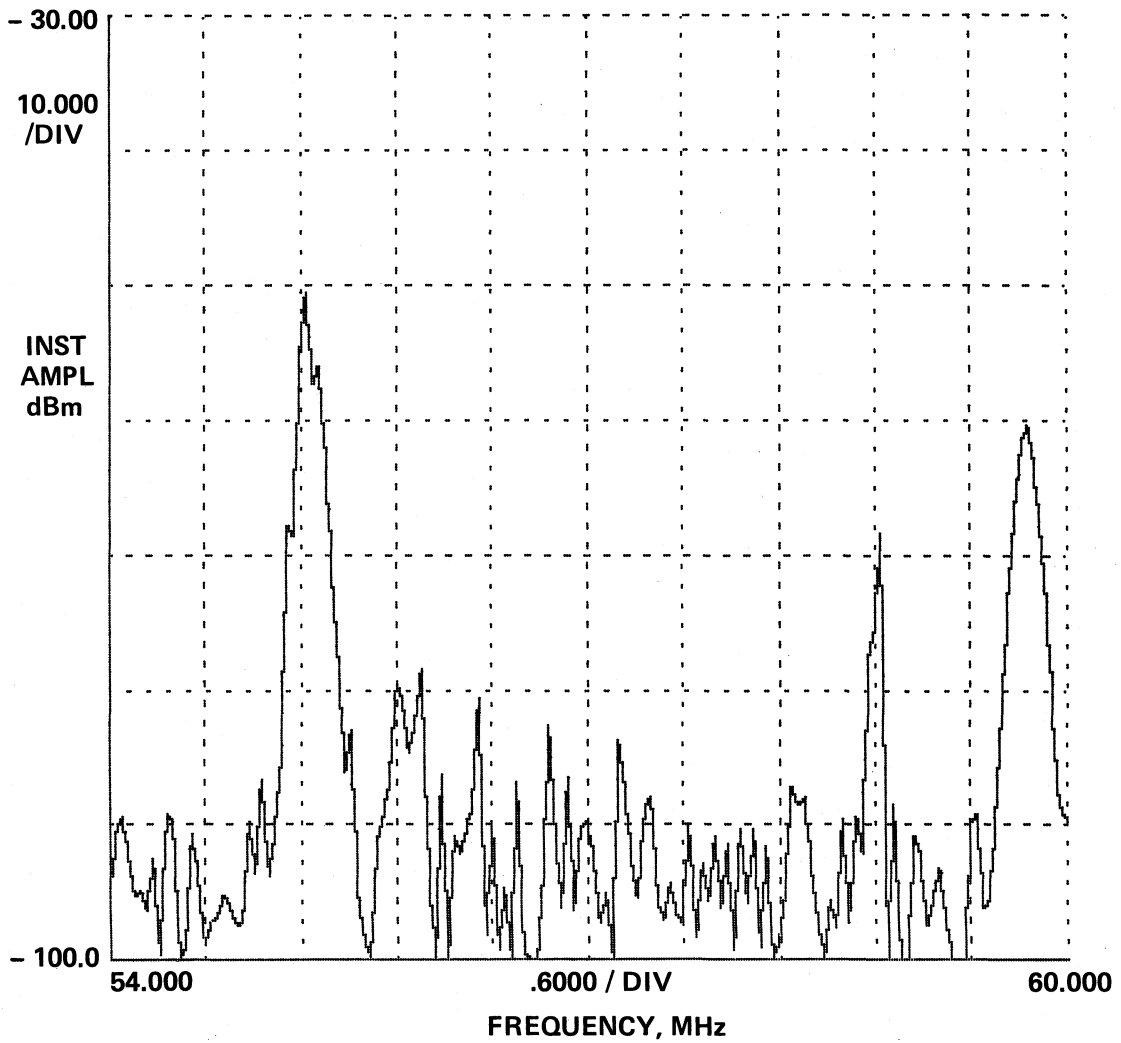


Figure 3. Television Channel 2 (KWGN) spectrum measured at 10th and Ford Street in Golden, Colorado.

CHANNEL 4 (10th & FORD, GOLDEN, COLO.)

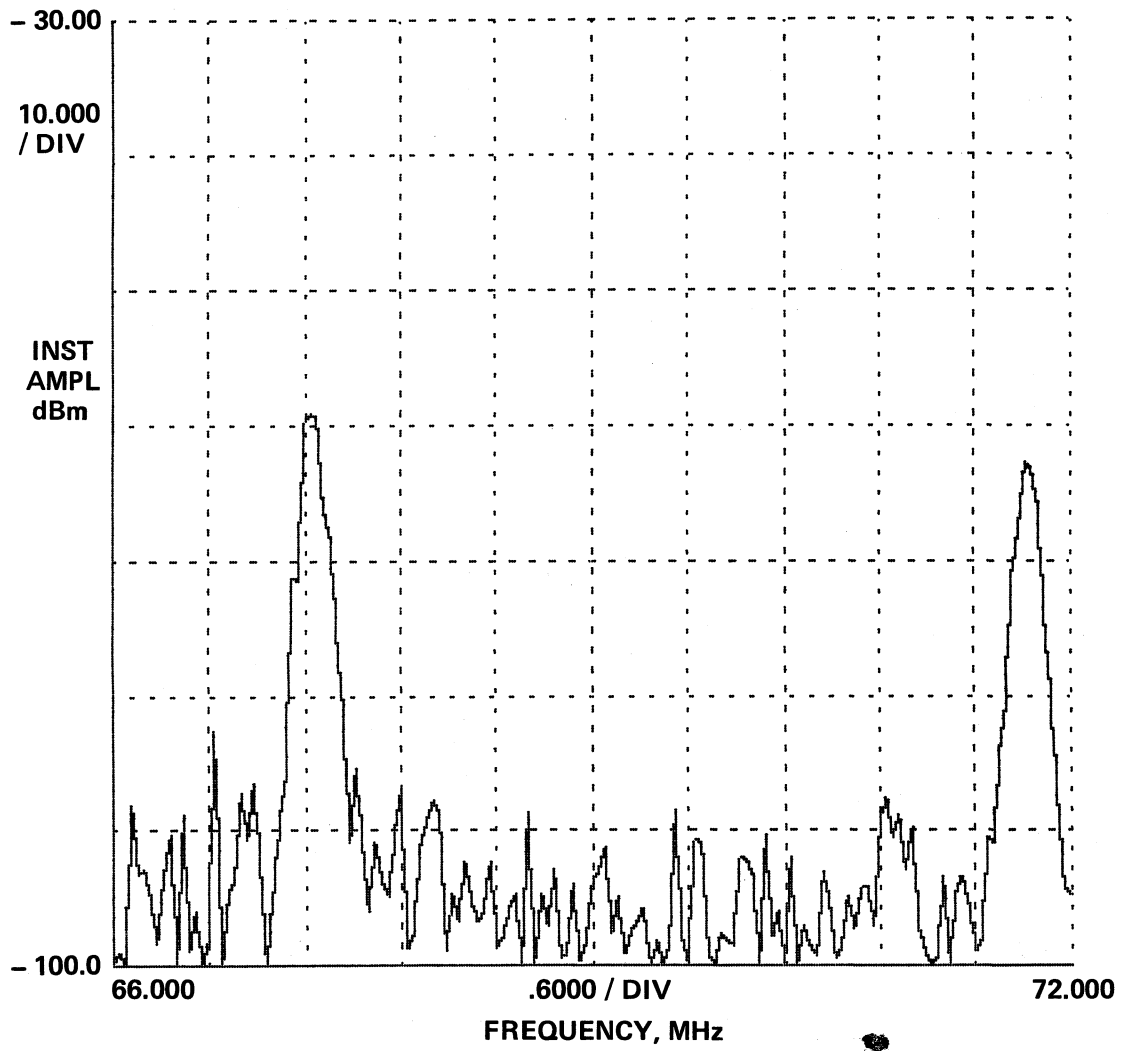


Figure 4. Television Channel 4, (KOA) spectrum measured at 10th and Ford Street in Golden, Colorado.

CHANNEL 7 (10th & FORD, GOLDEN, COLO.)

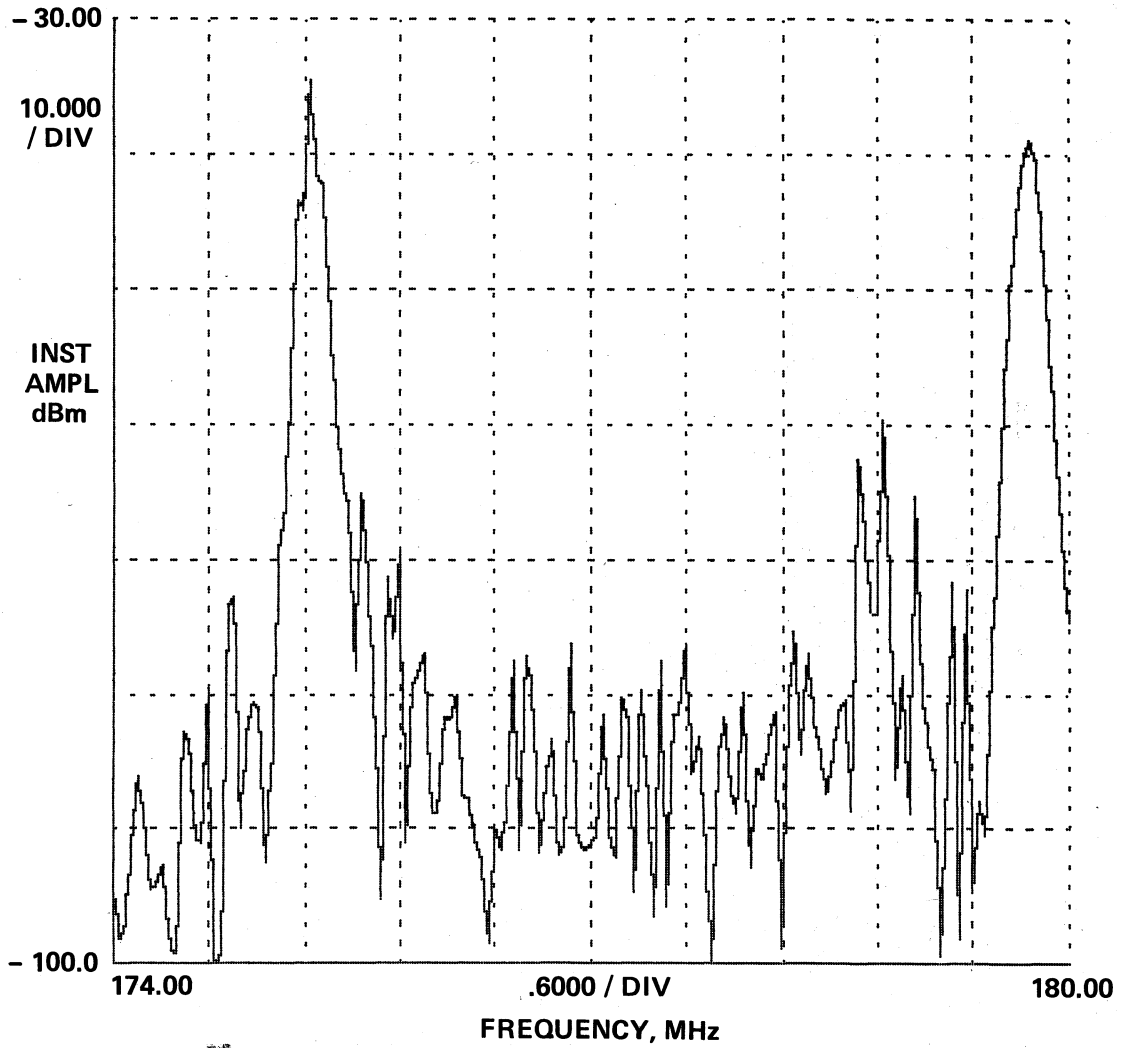


Figure 5. Television Channel 7 (KMCH) spectrum measured at 10th and Ford Street in Golden, Colorado

CHANNEL 9 (10th & FORD, GOLDEN, COLO.)

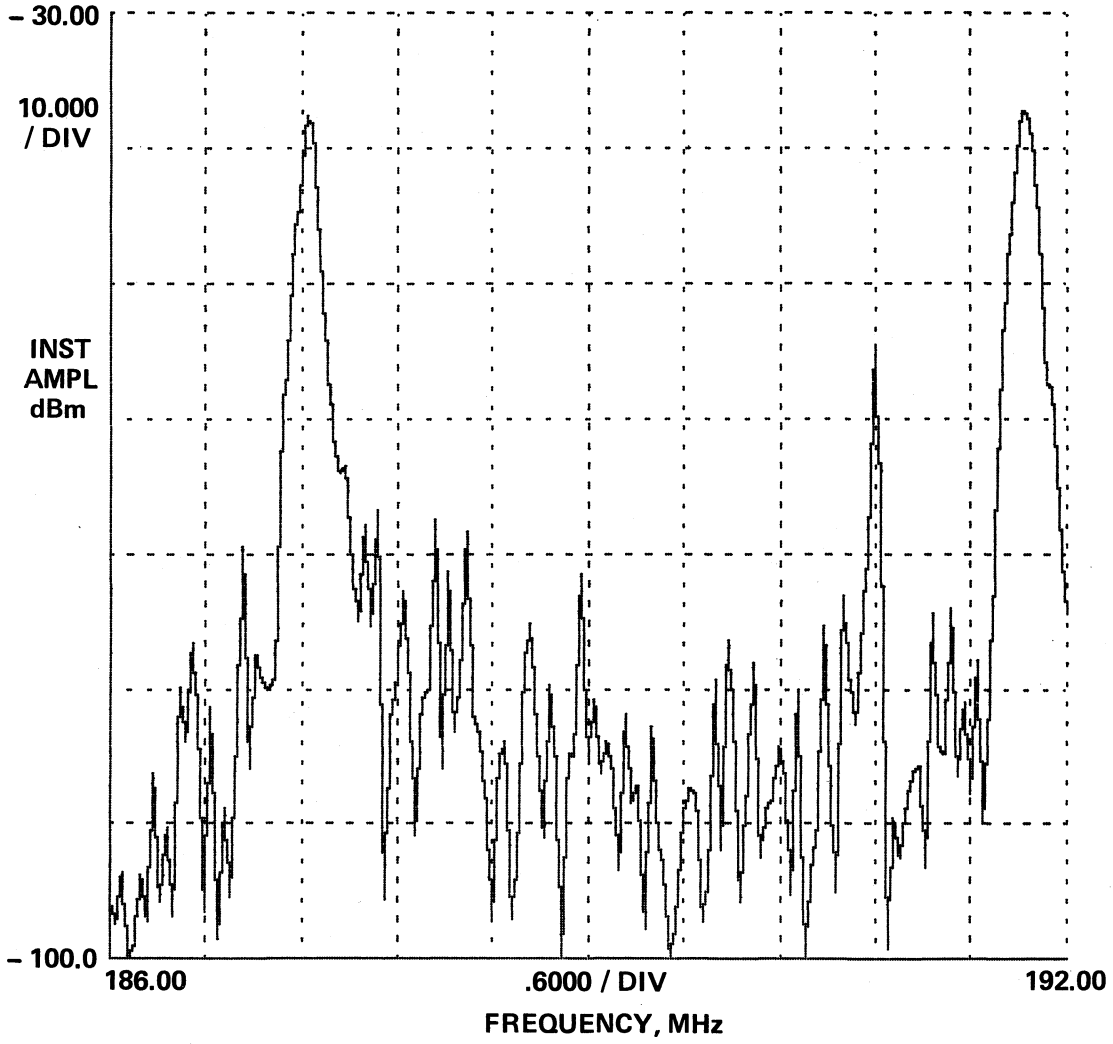


Figure 6. Television Channel 9 (KBTU) spectrum measured at 10th and Ford Street in Golden, Colorado.

RECEIVED SIGNAL VARIATIONS AT 55.25 MHz (VIDEO) & 59.75 MHz (AUDIO) AT A
MOBILE SPEED OF 20 MPH EAST ON 44th St. IN GOLDEN, COLO.: TRANSMITTER
KWGN (Ch. 2), JUNE 6, 1979, RUN No. 11

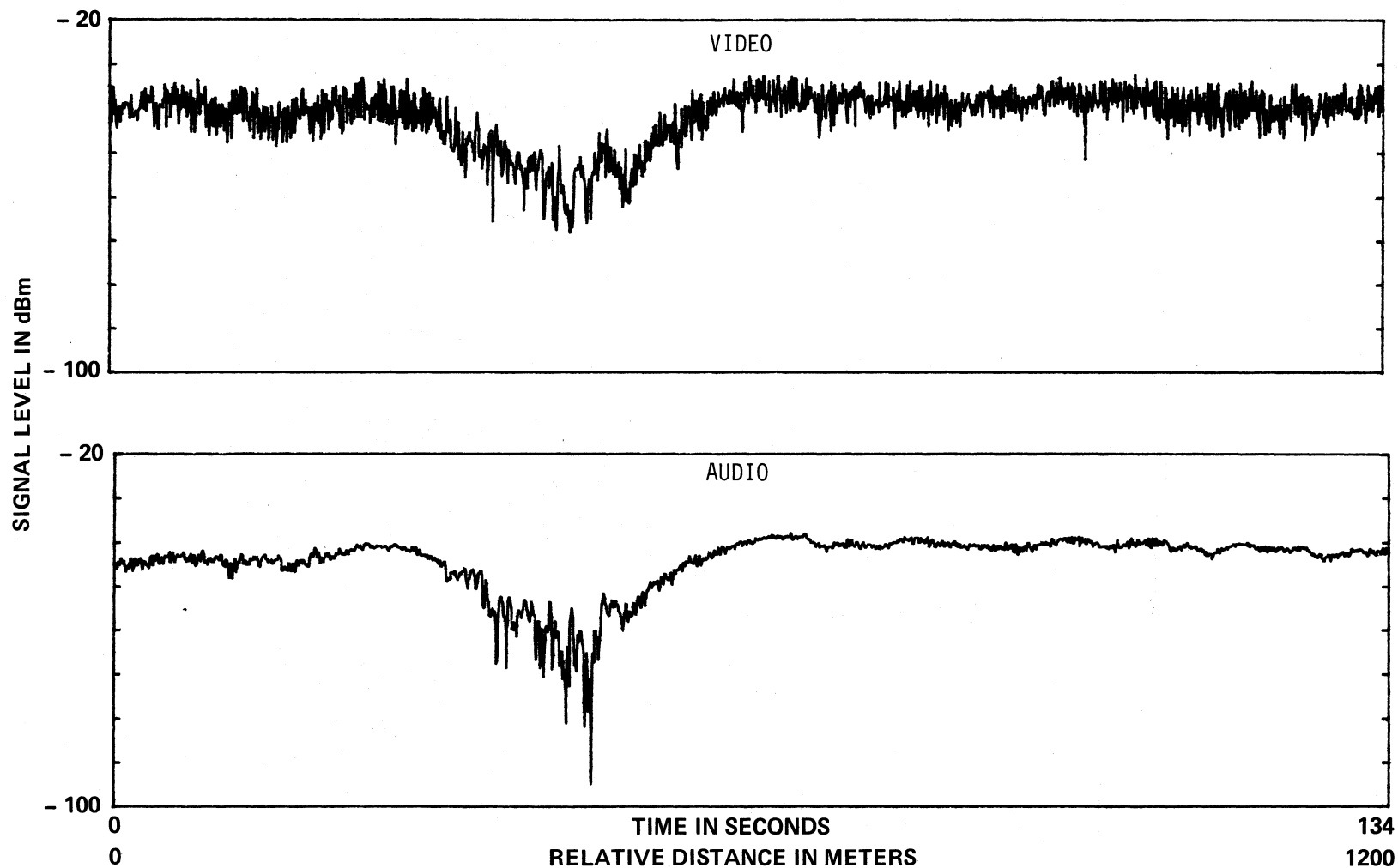


Figure 7. Typical signal variation of KWGN at a mobile speed of 20 mph. Run 11 on 6/6/79, East at 20 mph, Channel 2 at 55.25 MHz (video) and 59.75 MHz (audio).

RECEIVED SIGNAL VARIATIONS AT 67.24 MHz (VIDEO) & 71.74 MHz (AUDIO) AT A
MOBILE SPEED OF 20 MPH EAST ON 44th St. IN GOLDEN, COLO.: TRANSMITTER
KOA (Ch. 4), JUNE 6, 1979, RUN No. 13

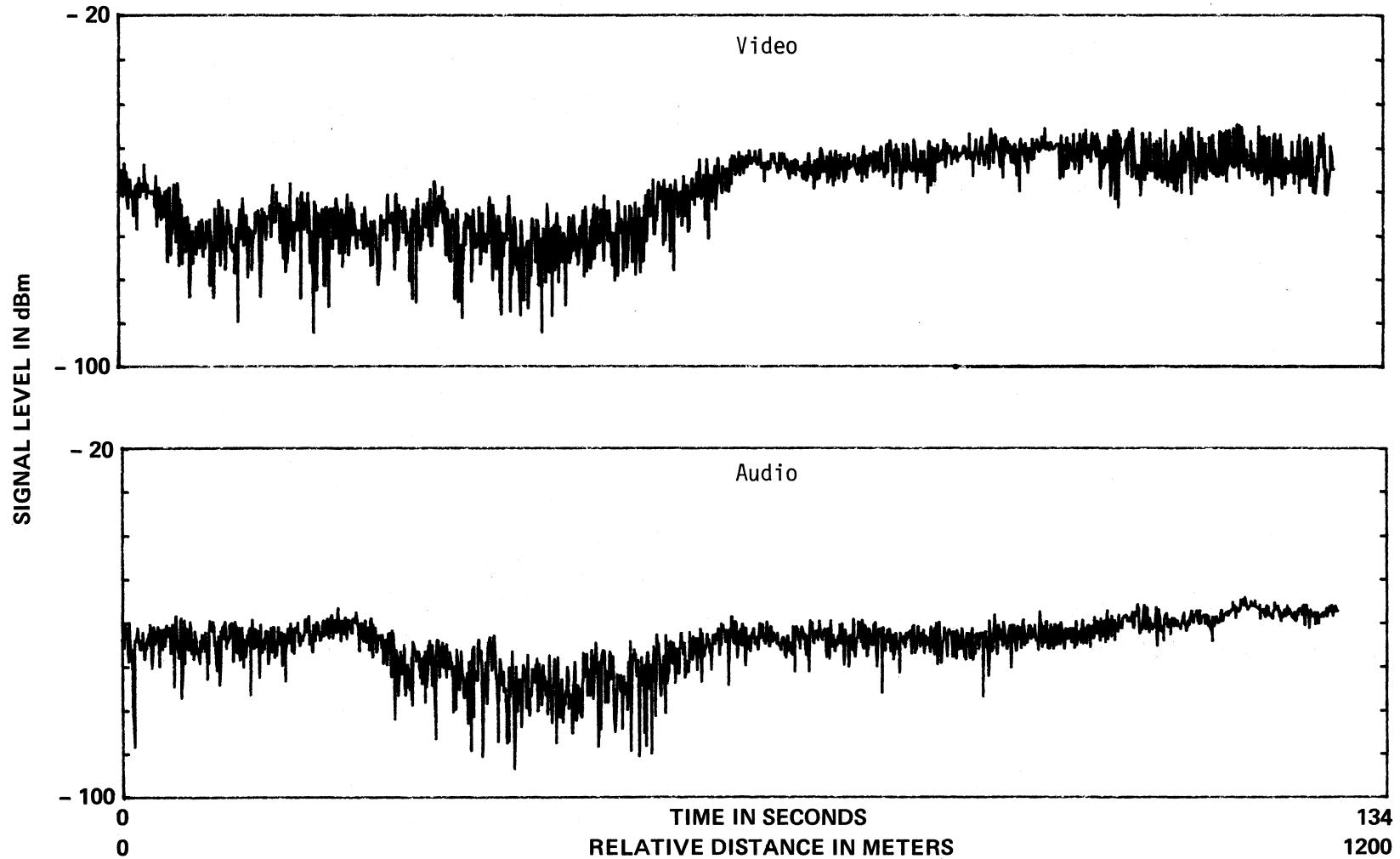


Figure 8. Typical signal variation of KOA at a mobile speed of 20 mph. Run 13 on 6/6/79, East at 20 mph, Channel 4 at 67.25 MHz (video) and 71.74 MHz (audio).

RECEIVED SIGNAL VARIATIONS AT 175.25 MHz (VIDEO) & 179.75 (AUDIO) AT A MOBILE SPEED OF 20 MPH EAST ON 44th St. IN GOLDEN, COLO.: TRANSMITTER KMGH (Ch. 7), JUNE 6, 1979, RUN No. 17

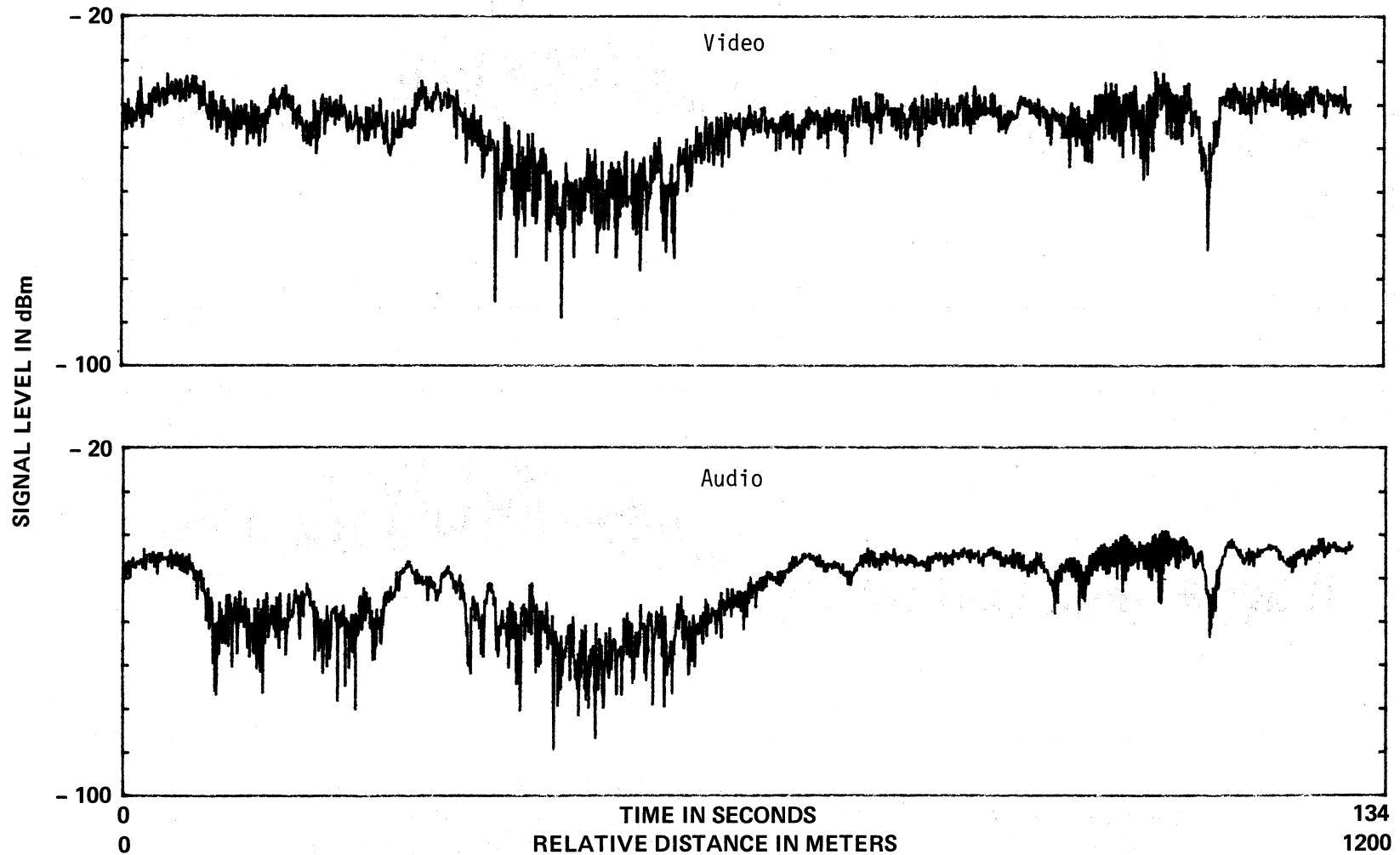


Figure 9. Typical signal variation of KMGH at a mobile speed of 20 mph. Run 17 on 6/6/79, East at 20 mph, Channel 7 at 175.25 MHz (video) and 179.75 MHz. (audio).

RECEIVED SIGNAL VARIATIONS AT 187.24 MHz (VIDEO) & 191.74 MHz (AUDIO) AT
A MOBILE SPEED OF 20 MPH EAST ON 44th St. IN GOLDEN, COLO.: TRANSMITTER
KBTV, 6 JUNE 1979

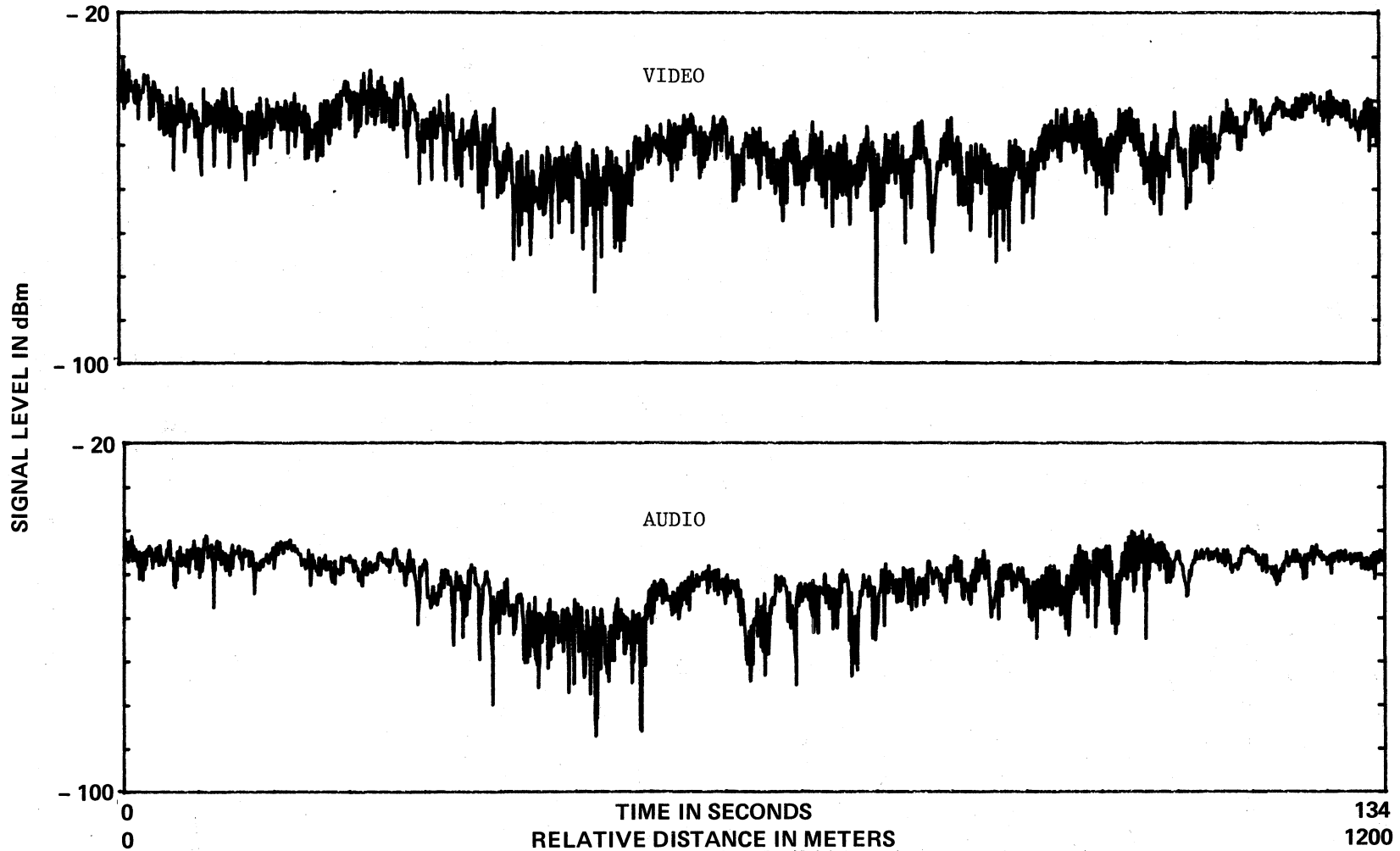


Figure 10. Typical signal variation of KBTV at a mobile speed of 20 mph. Run 15 on 6/6/79 going East at 20 mph on the 0.7 mile test course. Channel 9 (KBTV) at 187.24 MHz (video) and 191.74 MHz (audio).

3. THEORETICAL CONSIDERATIONS AND DATA ANALYSIS

The typical mobile communication configuration has one station fixed (in our case the TV transmitter) and the other moving, and the direct line of propagation between the transmitter and receiver will usually be obstructed by buildings or other man-made obstacles. Thus the secondary modes of propagation will be primarily by means of scattering from the sides of buildings, local terrain features, or diffraction around such obstacles. It is assumed in the statistical analysis that the received field is comprised of free space plane waves whose azimuthal angles of arrival occur at random for different positions of the receiver and whose phases are random. The phase and amplitude of each component can be assumed to be statistically independent. It is also usually assumed that at every point there are "n" component ($n > 3$) waves and that these "n" waves have the same amplitude (Norton, et al., 1955). Furthermore, it will be assumed that the transmitted wave is horizontally polarized and that the polarization is unchanged on scattering so that the received field is also horizontally polarized. Generally, the received field is a combination of the randomly scattered field and the direct wave when the receiver is within line-of-sight of the transmitter. There is also the possibility of having one or more specularly reflected waves which are comparable in amplitude to the direct wave (Dougherty, 1967). It will be shown that this combination of scattered and one or more coherent components is apparently the case for most of the data analyzed in this report.

3.1 Statistical Analysis of the June and July Data

If the scattered radiation field components are complex Gaussian random variables (phasors), then the signal envelope of these field components at the receiver antenna terminals will be Rayleigh distributed (Clarke, 1968). Then the Probability Density Function (PDF) of the envelope R will be Rayleigh,

$$q(R) = \frac{2R}{\sigma^2} \exp\left(-\frac{R^2}{\sigma^2}\right), \quad R \geq 0 \quad (1)$$

where σ is the mean value of R^2 , and the corresponding cumulative distribution function is

$$Q(R) = \int_R^{\infty} q(R) dR = \exp\left(-\frac{R^2}{\sigma^2}\right), \quad (2)$$

which graphs as a straight line of slope equal to -1 on "Rayleigh" paper.

A plot of the received field variations (signal envelope R) at 187.24 MHz (video) and 191.74 MHz (audio) for Run 15 on 6 June 1979 is shown in Figure 10. To test if these data follow a Rayleigh distribution, the histogram (approximation to the PDF) of the data was obtained (Figure 11) and then the percent probability that the data exceeded a given level was calculated and plotted on Rayleigh paper (Figure 12) to give the cumulative probability distribution. As can be seen from Figure 12, the distribution is "very nearly" Rayleigh. It will be shown later in the analysis that the observed deviation from a straight line (Rayleigh distribution function) can possibly be explained if it is assumed that the propagation medium produces two-component multipath plus a Rayleigh distributed signal. For comparison the CDF's are also plotted on a Gaussian scale (Figure 13). The correlation coefficients between the 191.74 MHz (audio) and 187.24 MHz (video) signals are plotted in Figure 14. A total of 1600 data points were used in computing the correlation coefficients.

In order to test the consistency of the experimental data, two data runs were made "back to back" on the 44th Avenue 0.7 mi test course. The first run was conducted going east (Run 15) away from the transmitter and the second run was made going west (Run 16) toward the transmitter. In order to test how similar Runs 15 and 16 were, the audio and video data of Run 15 were reversed and shifted 300 points to achieve maximum correlation with Run 16 and are plotted in Figure 15. The correlation coefficient between the east and west audio data for each run (the east and west runs were performed on opposite sides of the street), and for the east and west video data are plotted in Figure 16. At zero lag, the correlation coefficient for the audio signals (≈ 0.7) is greater than that for the video signals (≈ 0.6). This would appear to indicate that there are time variations in the data as well as space variation. This nonstationary character of the data makes the analysis and interpretation of the results difficult but if one performs a spectral analysis, considerable insight into the nature of the fading mechanism can be gained as will be shown in the next section.

3.2 Power Spectrum Analysis

In order to investigate the nature and causes of the fading characteristic of the signal envelope, which is a band-limited time-varying function, it is useful to examine the power spectrum. One can thus determine the distribution and extent of the energy in the band, and hopefully identify the probable causes of the observed fading. The power spectra of the signals were obtained by taking the

HISTOGRAM FOR RUN No. 15, ON JUNE 6, 1979

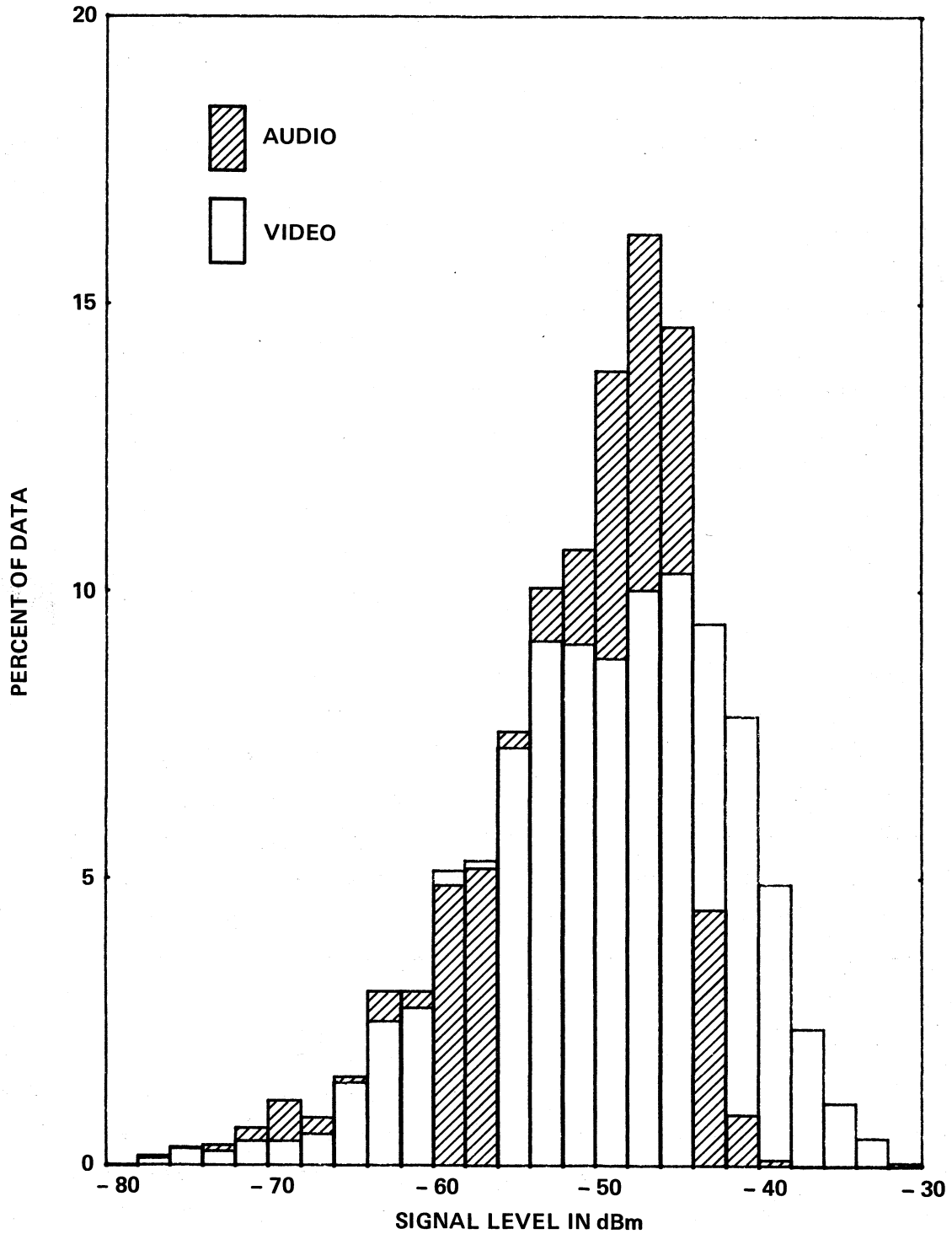


Figure 11. The relative frequency diagram which is an approximation to the probability density function for the data of Run 15.

RUN No. 15 EAST ON 44th St. AT 20 MPH 6 JUNE, 1979

CUMULATIVE PROBABILITY DISTRIBUTIONS FOR 187.24 MHz (VIDEO)
& 191.74 MHz (AUDIO) RAYLEIGH DISTRIBUTION FUNCTION SCALE

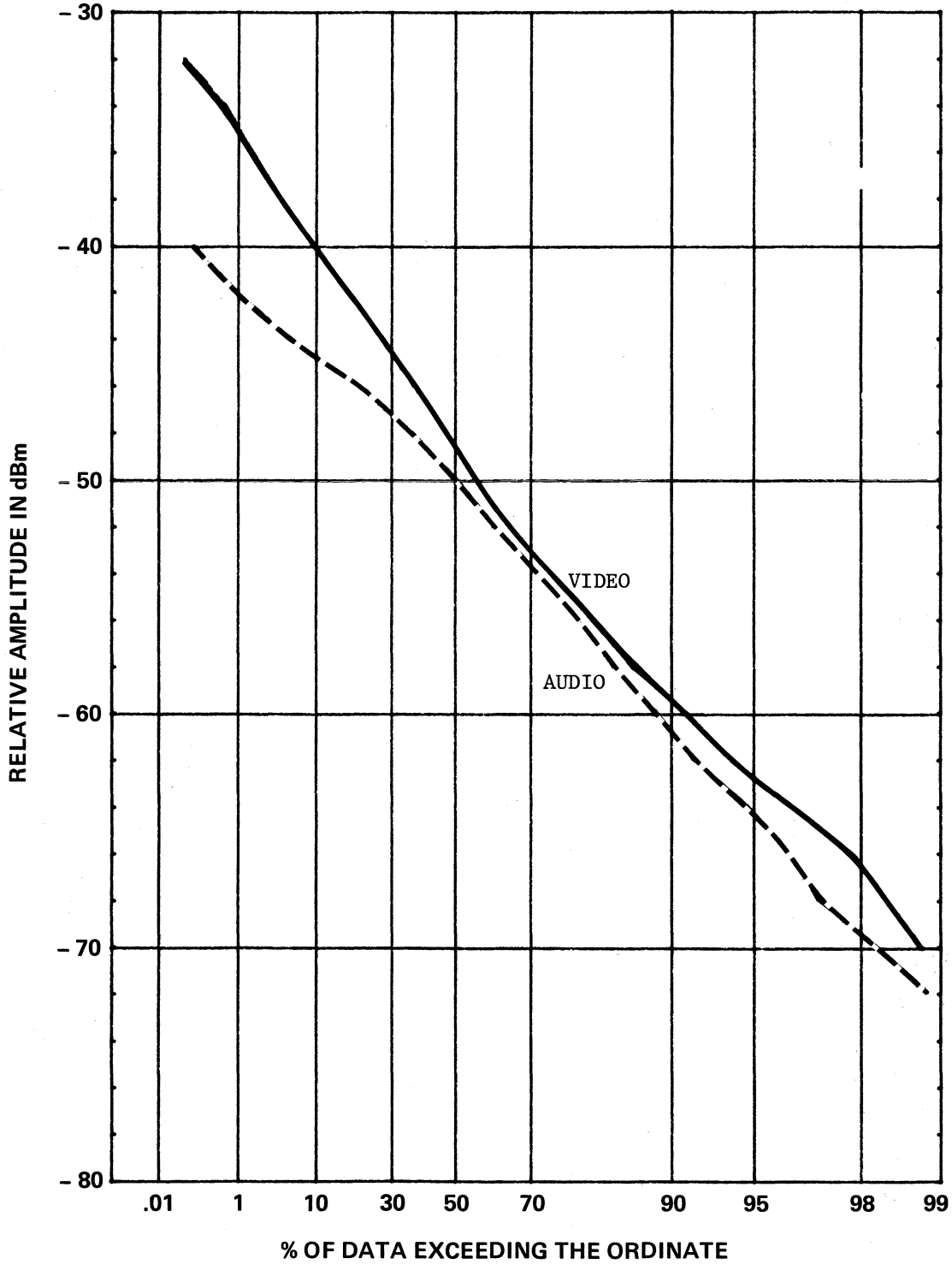


Figure 12. Cumulative probability distribution for the data of Run 15 plotted on Rayleigh paper.

RUN No. 15 EAST ON 44th St. AT 20 MPH 6 JUNE, 1979

CUMULATIVE PROBABILITY DISTRIBUTIONS FOR 187.24 MHz (VIDEO)
& 191.74 MHz (AUDIO) GAUSSIAN DISTRIBUTION FUNCTION SCALE

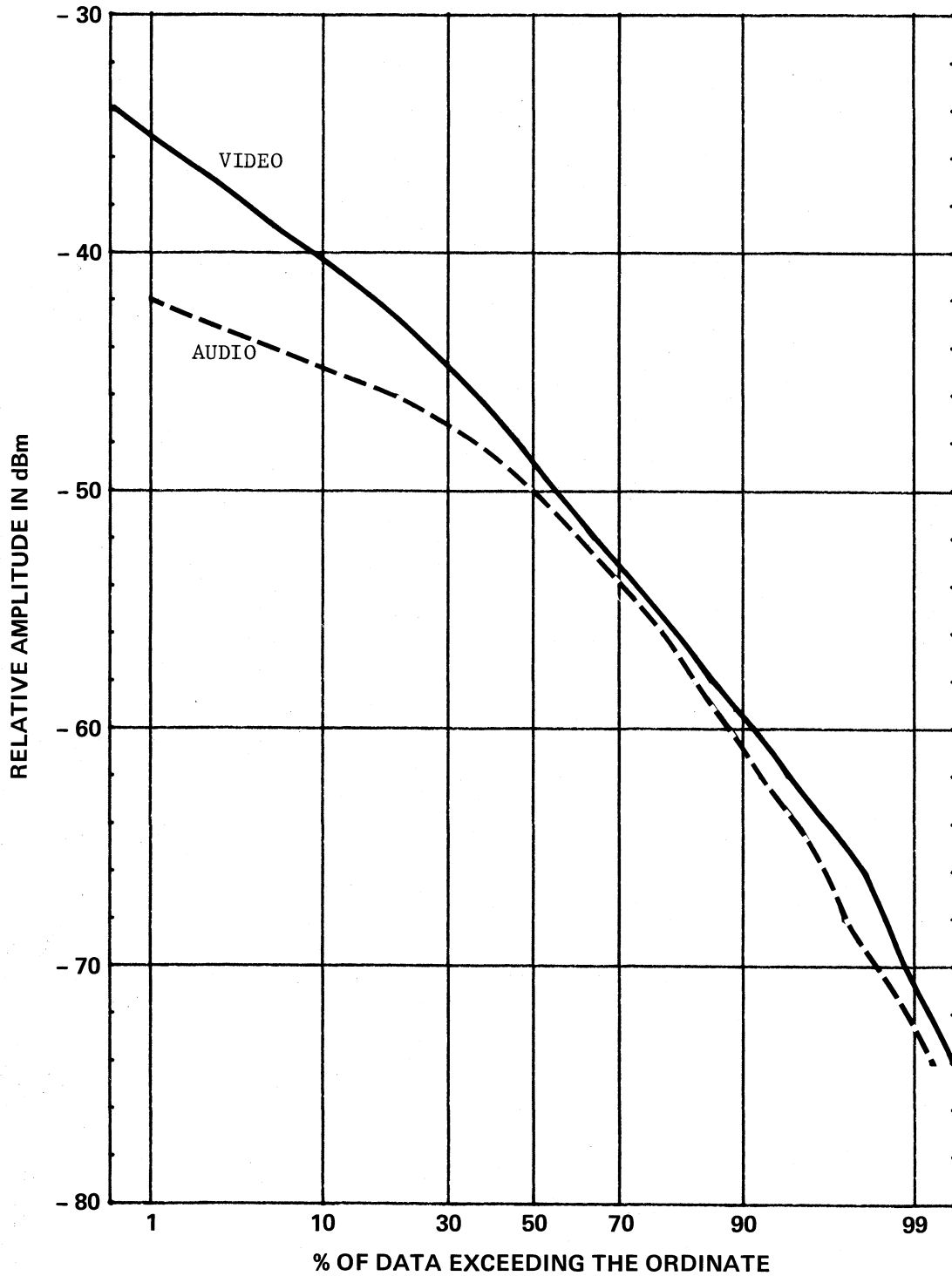


Figure 13. Cumulative probability distribution for the data of Run 15 plotted on Gaussian paper.

CORRELATION COEFFICIENT FOR RUN 15 AUDIO & VIDEO

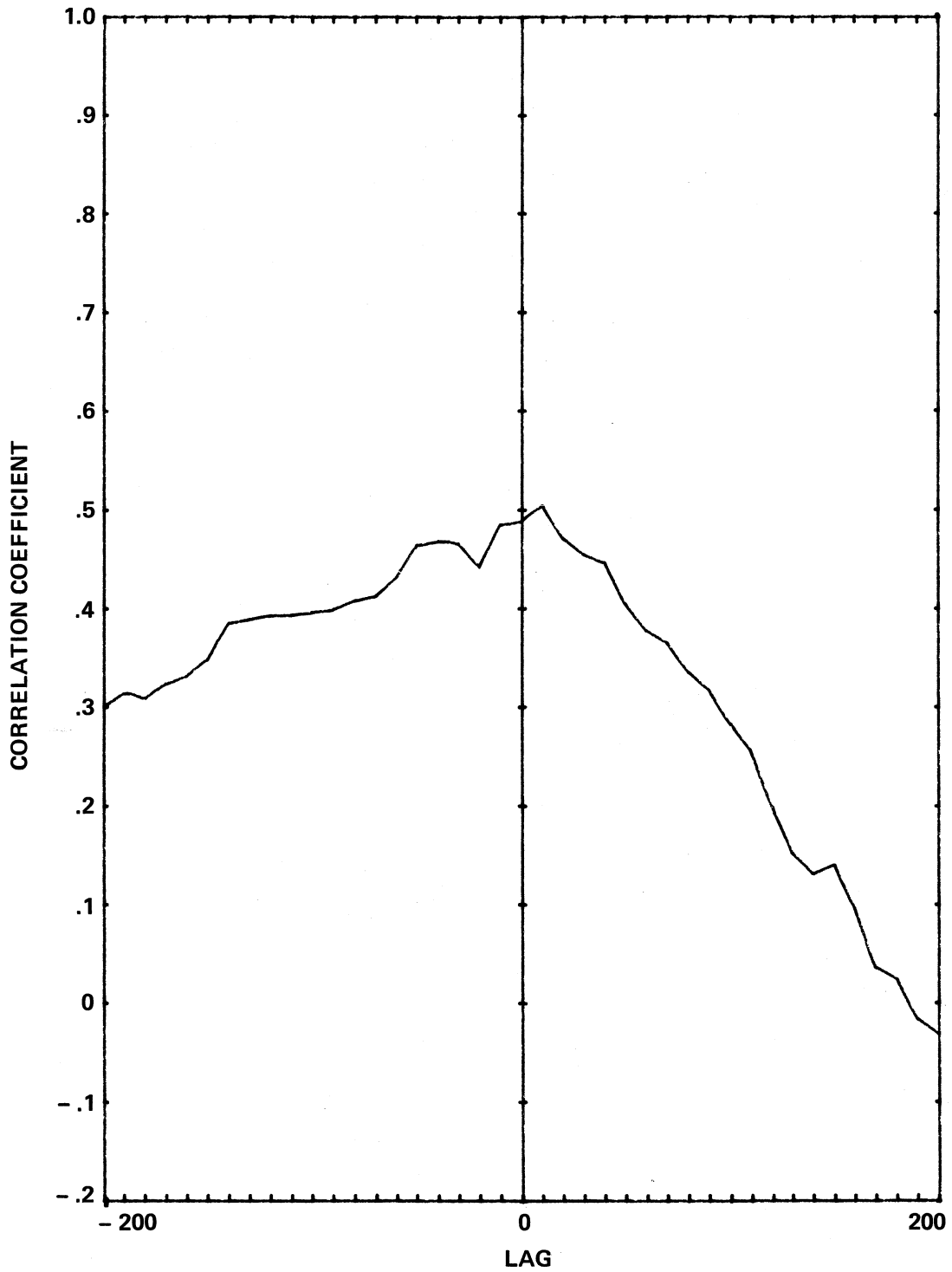
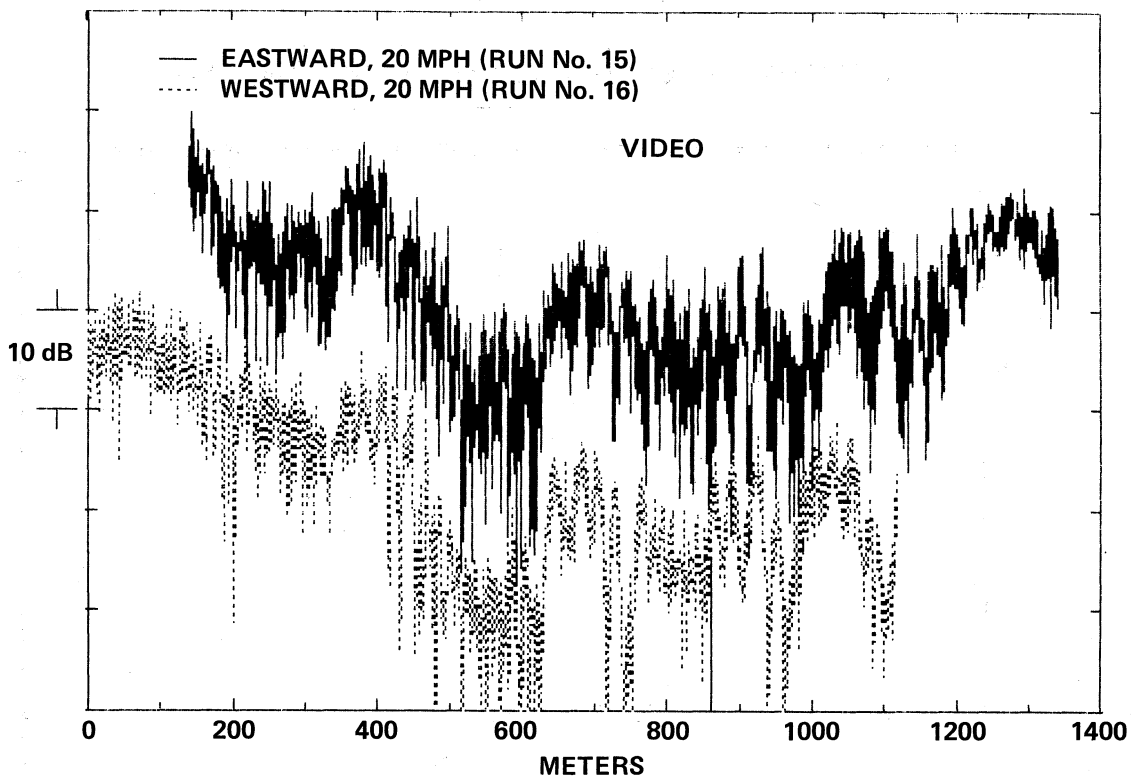


Figure 14. Correlation coefficient between the audio and video signals for Run 15.

SIGNAL ENVELOPES OF EAST - WEST RUNS
JUNE 6, 1979



SIGNAL ENVELOPES OF EAST - WEST RUNS

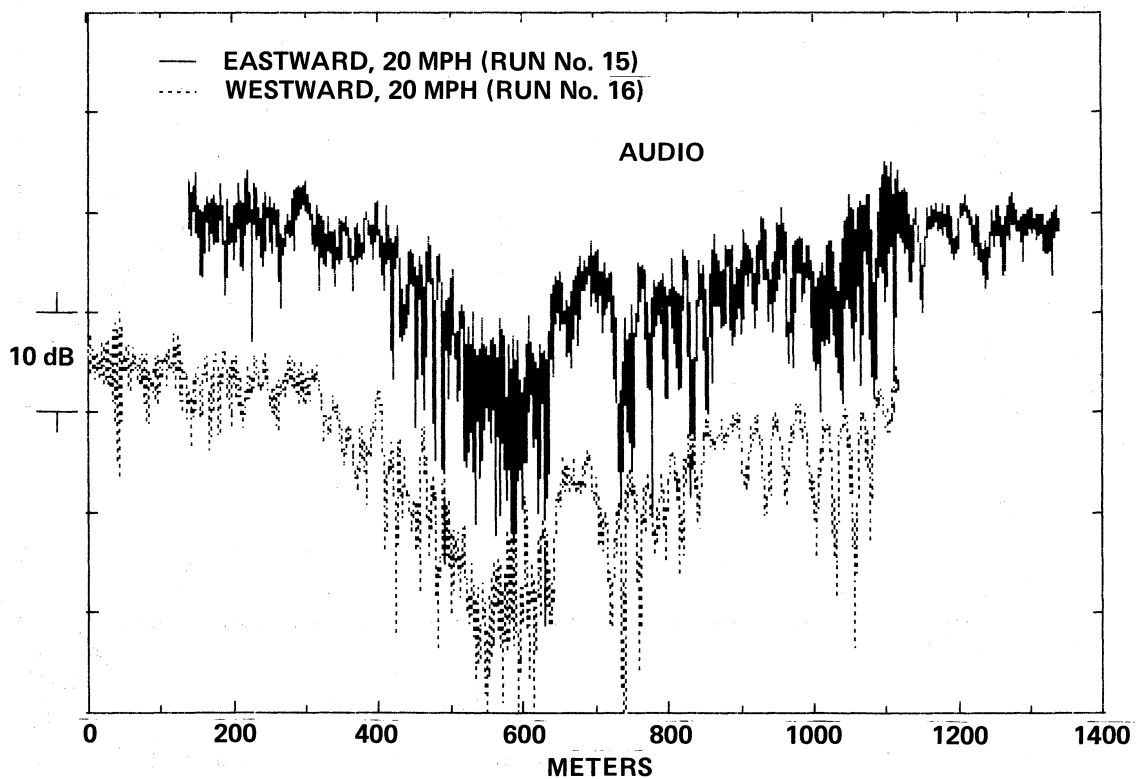


Figure 15. Signal envelope for Runs 15 and 16 with Run 15 reversed and shifted 300 points.

CORRELATION COEFFICIENT FOR EAST-WEST VIDEO & AUDIO

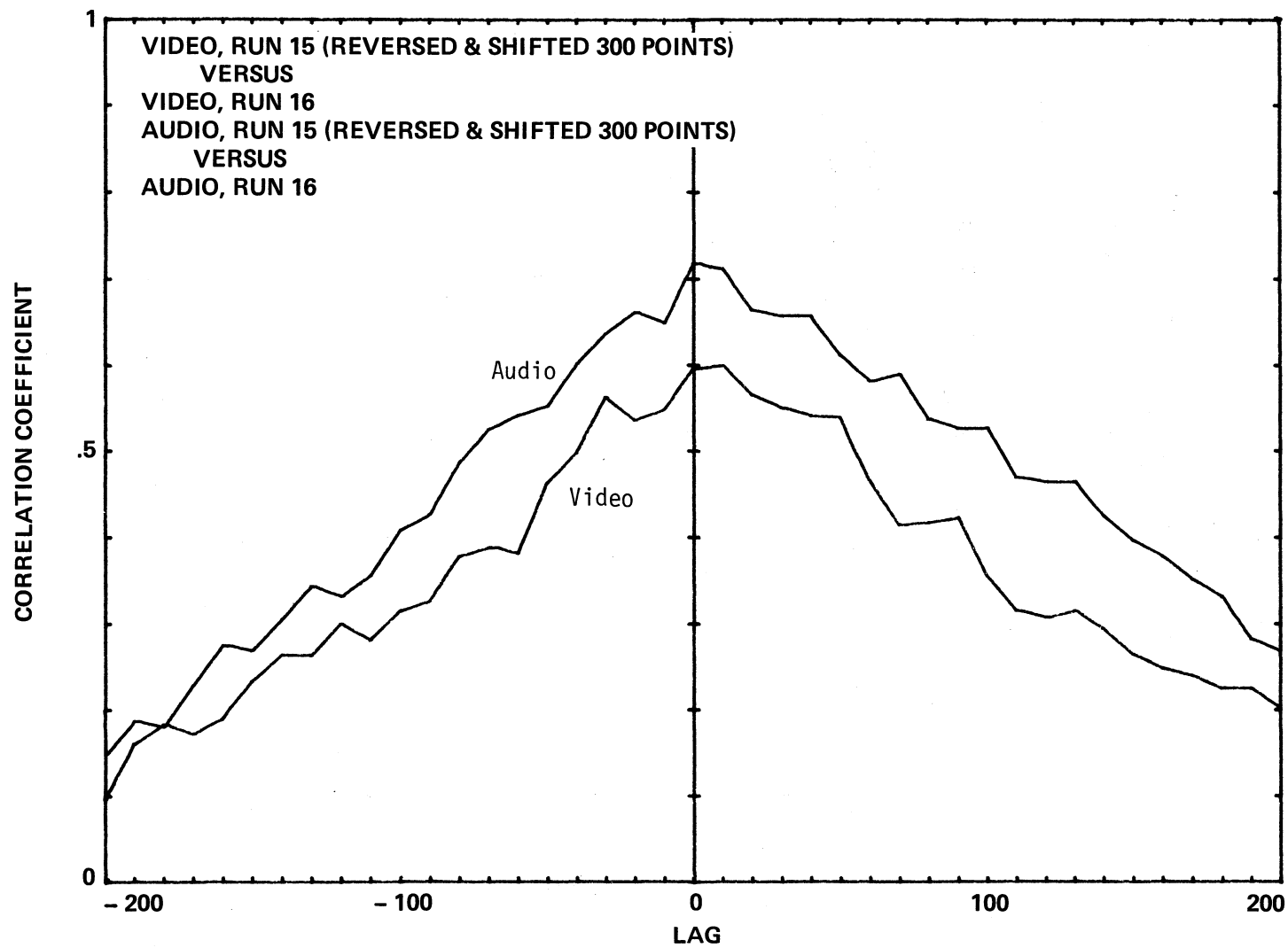


Figure 16. Correlation coefficients for Runs 15 and 16.

SPECTRAL DENSITY IN $(\text{dBm})^2 / (\text{METER})^{-1}$
VERSUS
INVERSE DISTANCE IN $(\text{METERS})^{-1}$

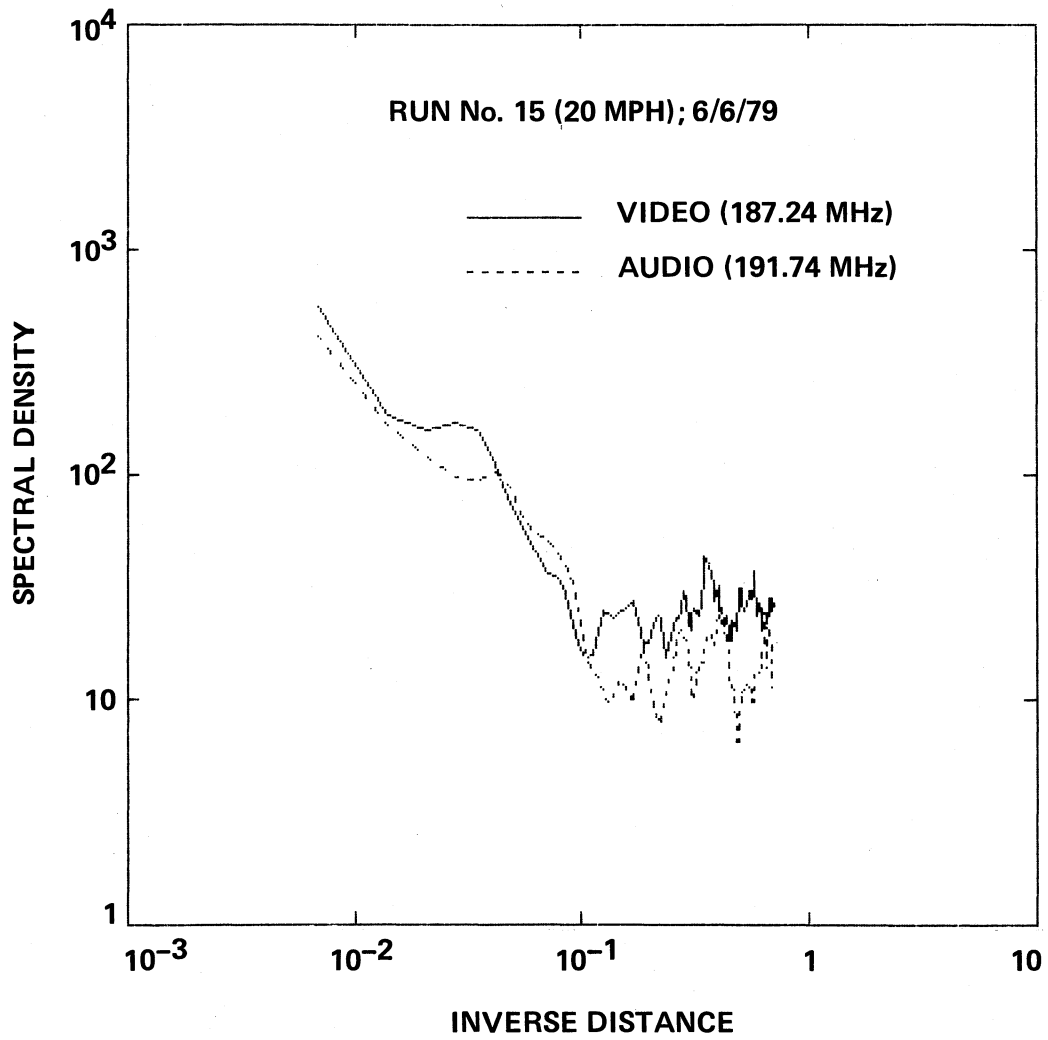


Figure 17. Power spectra for Run number 15 for video and audio data at 20 mph.

SPECTRAL DENSITY IN $(\text{dBm})^2 / (\text{METER})^{-1}$
VERSUS
INVERSE DISTANCE IN $(\text{METERS})^{-1}$

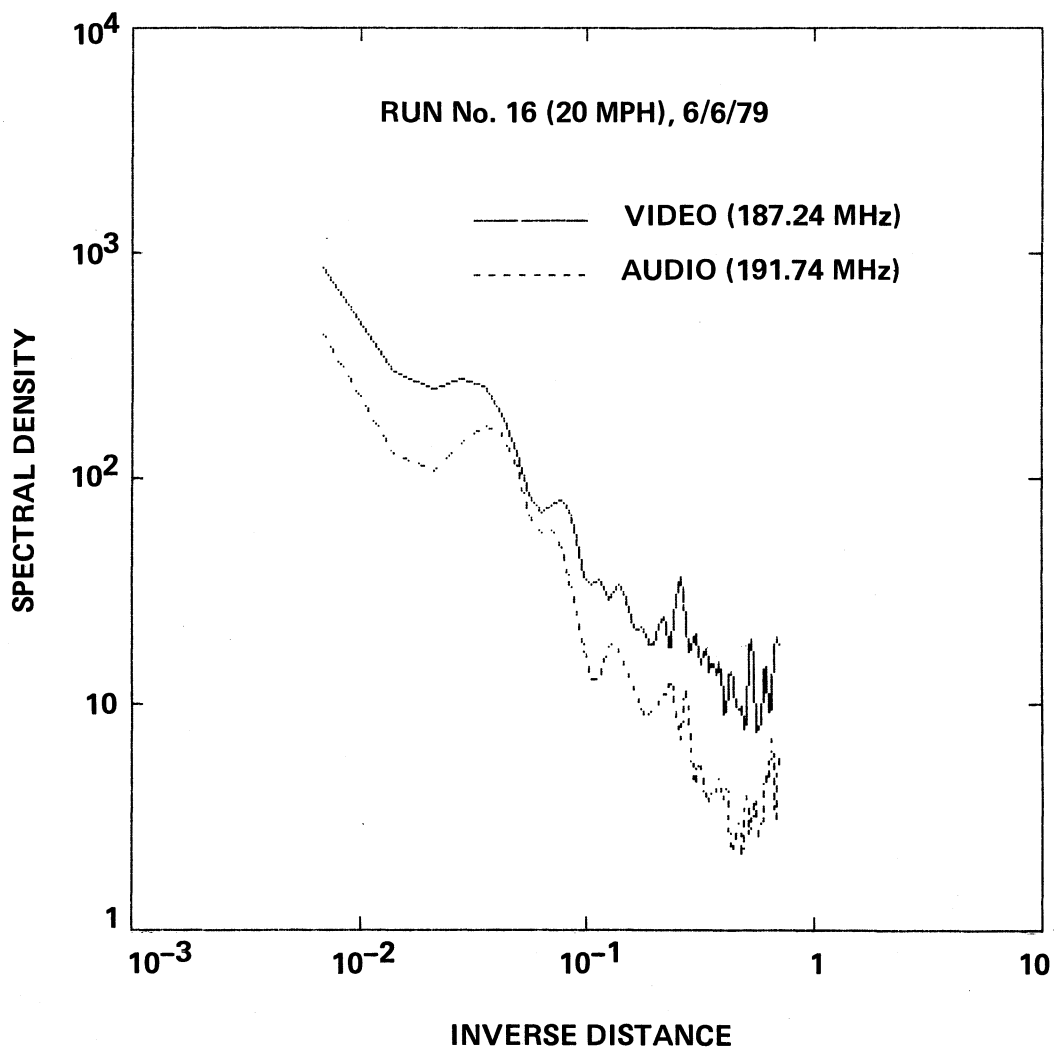


Figure 18. Power spectra for Run number 16 for video and audio data at 20 mph.

Fourier transform of the autocovariance function of the input time series (Blackman and Tukey, 1958) and are shown for Runs 15 and 16 in Figures 17 and 18. (Appendix).

By calculating the spectral density as a function of inverse distance, the data were normalized to a spatial variation. This was accomplished by converting the data sample spacing in seconds ($\Delta t = 0.08$ sec) to a distance spacing in meters ($\Delta d = 0.72$ meters at 20 mph), and then calculating the power spectrum. This effectively "normalizes" the data for vehicle speed, and thus only the distance traveled by the measurement vehicle is used as the independent variable. The spectral density is then given in units of $(\text{dBm})^2/(\text{meter})^{-1}$ as a function of inverse distance (wave number) in m^{-1} . From Figure 18, it can be seen that there are three fairly distinct "lines" in the spectrum at approximately 0.04, 0.08, and 0.16 m^{-1} which correspond to fading rates of 0.36, 0.72, and 1.43 Hz or vehicle travel distances of 25.0, 12.5, and 6.25 meters, respectively.

In order to verify that these "lines" in the energy spectrum are real, an additional experiment was conducted on 24 July 1979 using vehicle speeds of 30, 20, and 10 mph on the same 0.7 mi course in Golden. The plot of Spectral Density versus Inverse Distance shown in Figure 19 summarizes the results of the video data taken going west at 30, 20, and 10 mph. As can be seen from the figure, both the 20 and 30 mph data show the three spectral peaks and in the same place as the 6 June data discussed earlier. The 10 mph data shows only one spread out peak since the vehicle velocity at 10 mph is not fast enough to separate the three fades.

It can be shown that this fading is due to the beating within the receiver of different carrier frequencies arising from the different Doppler shifts occurring for the directly incident and reflected waves (Ossanna, 1964).

3.3 Doppler Fading and Standing Waves

A model based on the reflection geometry from nearby randomly located vertical plane reflectors was used by Ossanna (1964) to show that both the standing wave pattern and the Doppler shift mechanism for fading give nearly identical results. However, the Doppler shift mechanism has the added advantage that it is easier to see what fade rates will occur when more than one reflector is involved. When m reflectors are simultaneously effective, there can be $m(m+1)/2$ beat frequencies observed. Conversely, by observing the number of peaks in the power spectrum, one can deduce the number of principal reflectors present. Thus, for the 0.7 mi course, there are three peaks and therefore two principal interfering waves in addition to the Rayleigh distribution, which could account for the deviation from Rayleigh shown in the cumulative probability distribution plot (Figure 12).

SPECTRAL DENSITY IN $(\text{dBm})^2 / (\text{METERS})^{-1}$
VERSUS
INVERSE DISTANCE IN $(\text{METERS})^{-1}$

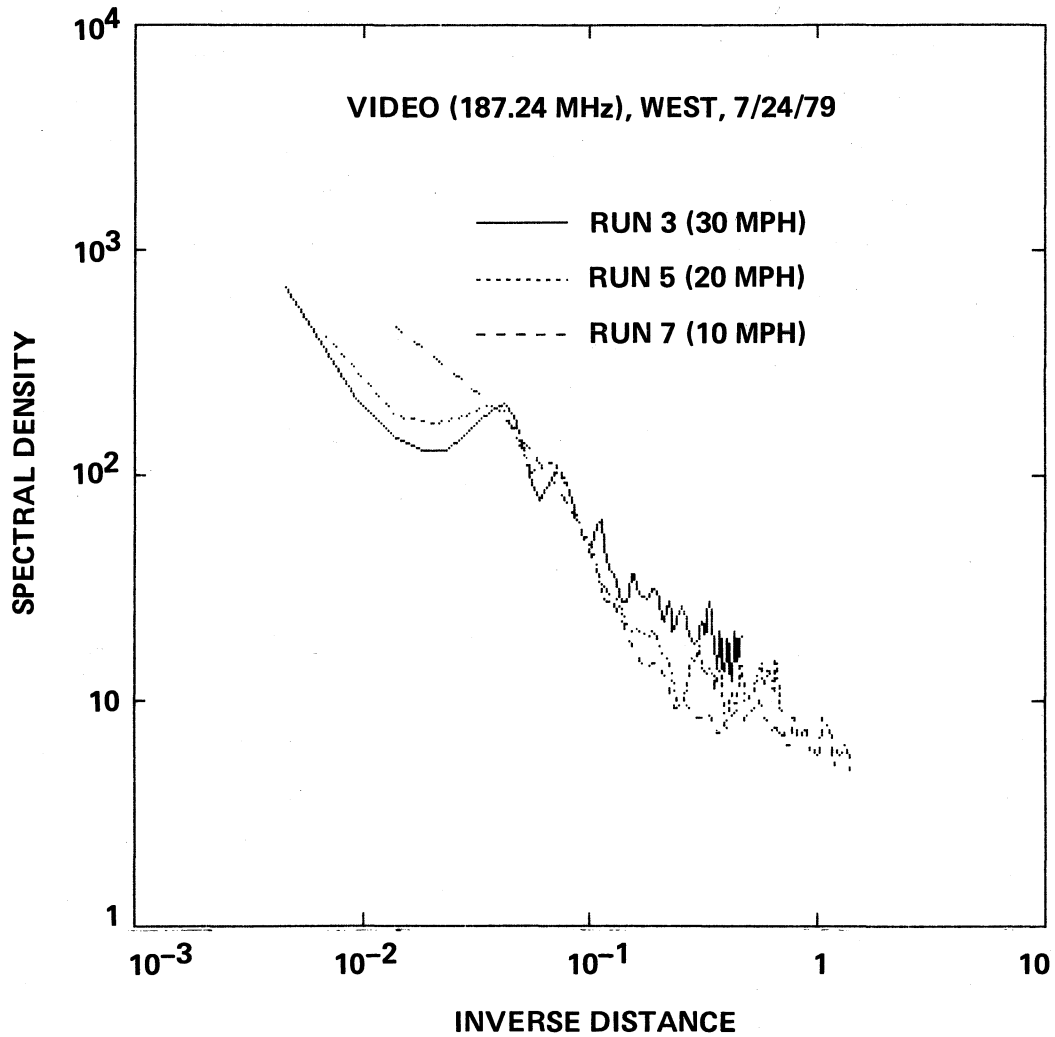


Figure 19. Composite plot of West bound Channel 9 (KBTU) video data power spectrum at 10, 20, and 30 mph.

All of the data discussed thus far was obtained on the 0.7 mi course where most of the EM energy arrived at the receiver by a number of indirect paths (the scattered field). In order to obtain a sampling of the signal distribution in the Denver metropolitan urban area where the field would generally be a combination of a scattered field with a direct wave, additional measurements of the Channel 9 Video Signal (187.24 MHz) were conducted on 14 August 1979 along the dashed route shown in Figure 1. These measurements were made in 52 segments of approximately 50 yards at 0.5 mi increments along the route. One thousand measurements were taken during each 50 yard segment. The vehicle speed was 40 mph and the sampling rate was one per every 3 milliseconds. Typical samples of the signal variations are displayed in Figures 20 through 22. The related power spectrum for each of these runs is given in Figures 23 through 25. As expected, there is a pronounced peak in the spectrum near 1 (meter)^{-1} , due to the standing wave pattern set up by the direct line-of-sight wave from the transmitter on Lookout Mountain and a reflected wave from directly in front of the measurement van (probably due to a large concrete and steel overpass directly perpendicular to the direction of travel). It is not fully understood what mechanism causes the variations in the high wave number portion of the spectrum; however, it is thought that they are possibly due to a combination of weak specularly reflected waves from nearby buildings and other moving vehicles that were present on both sides of the road when the measurements were performed.

3.4 Statistical Analysis of the August Data

It is likely from the cumulative probability distribution analysis of the 52 data segments obtained along the 30 mi route shown in Figure 1 that the probability density distribution is not "Rayleigh." The slope of the cumulative distribution function (CDF) for each data segment varies from approximately -0.3 to -1.2 along the measurement route. A composite sample of this variation is shown in Figure 26 for segments 1, 4, 5, and 24. Segment 24 with a slope of -1.015 was obtained along the Valley Highway portion of the data run and is the closest to a Rayleigh distribution of all the measurements made on 14 August 1979, although several of the other segments along this portion of the run were also very nearly Rayleigh.

We are thus led to the conclusion that whenever there are strong specular reflections and the main beam of the transmitting antenna is present, the cumulative distribution function will deviate from a straight line and the probability density function (PDF) would have to be considered an approximation to a Weibull model (Weibull, 1951) with the PDF given by

6TH AVE., VALLEY HWY., I-70 LOOP. 8/14/79

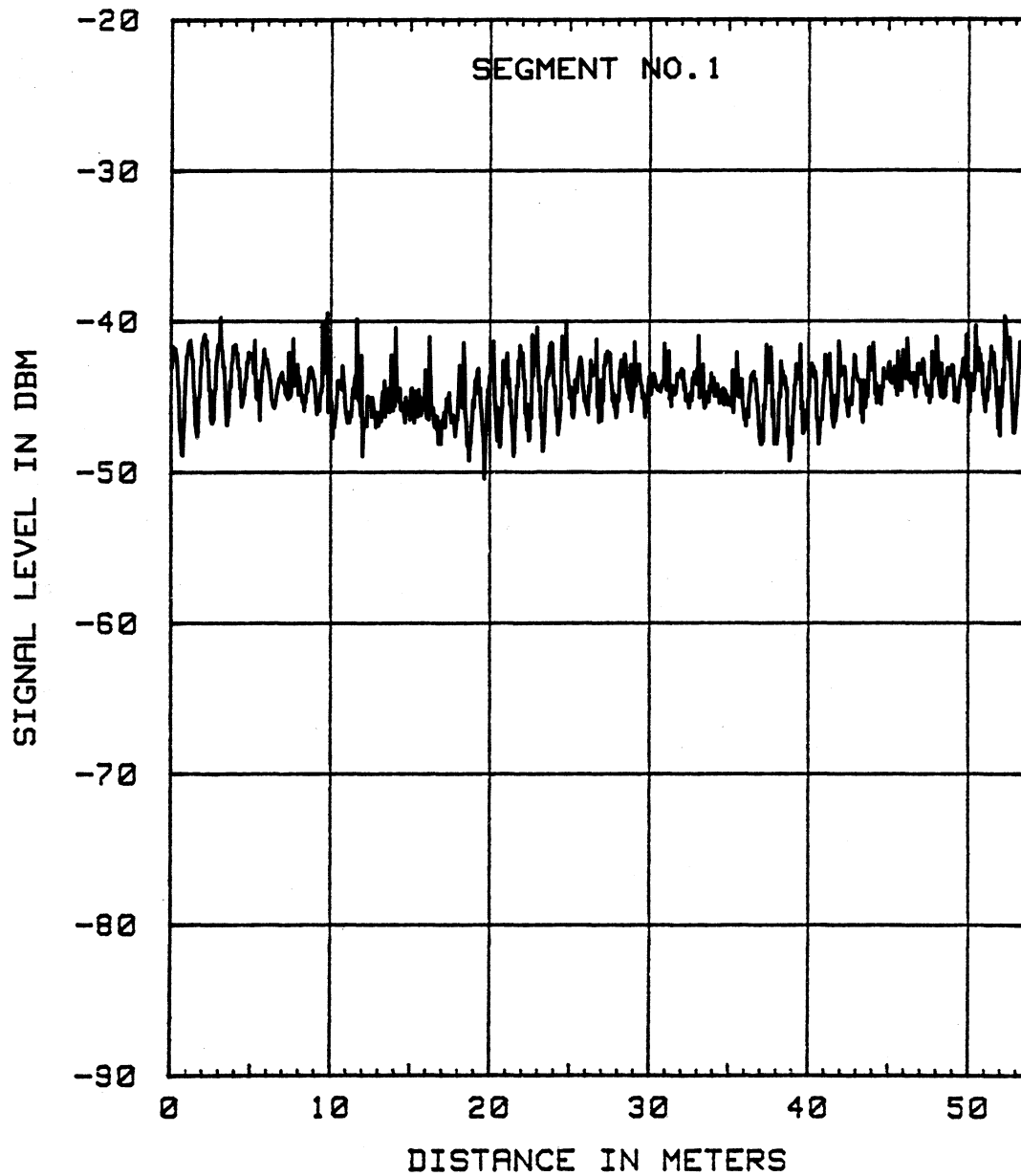


Figure 20. 14 August '79 data for segment number 1, Channel 9 (KBTv) at 187.24 MHz (Video).

6TH AVE., VALLEY HWY., I-70 LOOP. 8/14/79

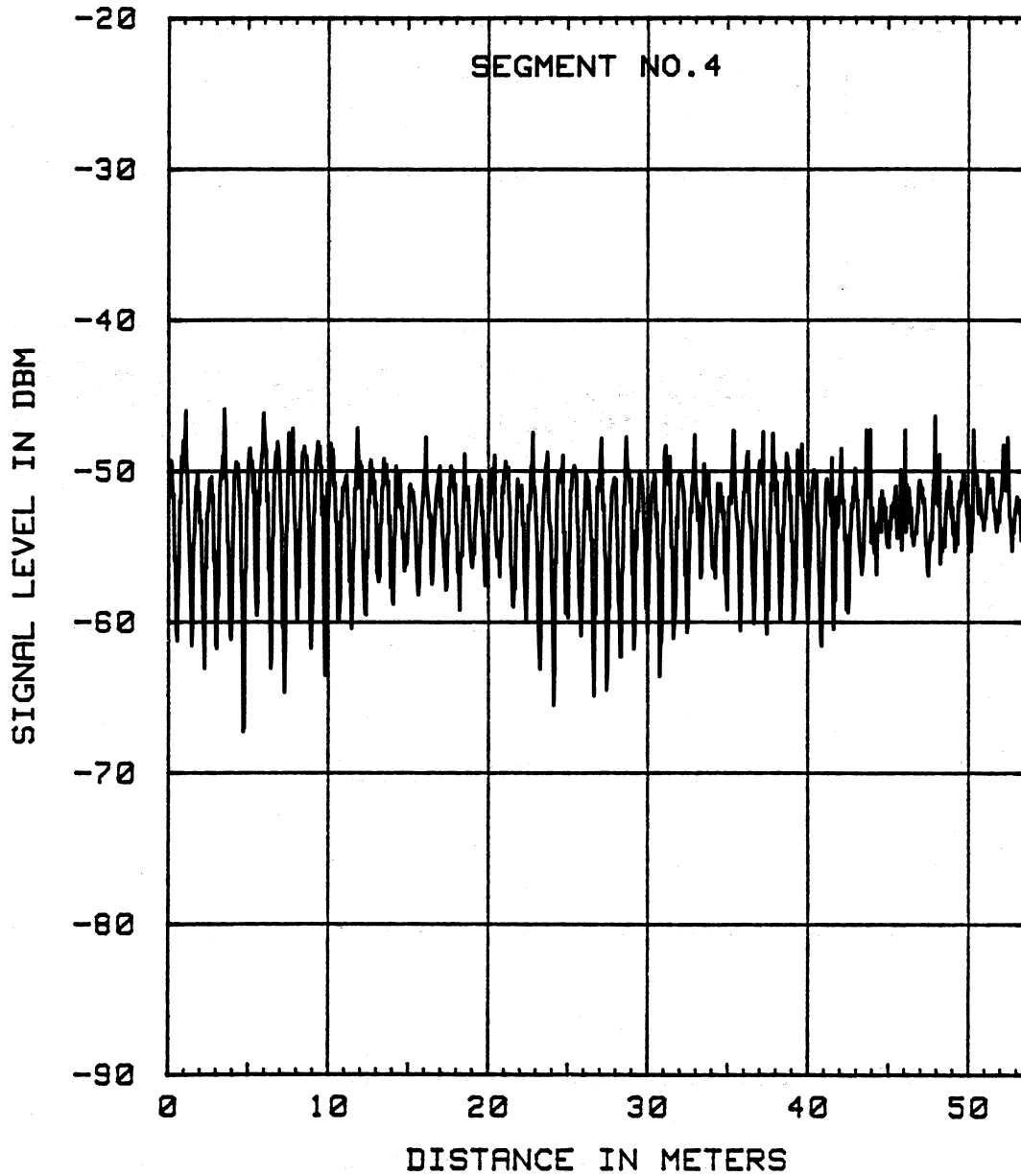


Figure 21. 14 August '79 data for segment number 4, Channel 9 (KBTv) at 187.24 MHz (Video).

6TH AVE., VALLEY HWY., I-70 LOOP. 8/14/79

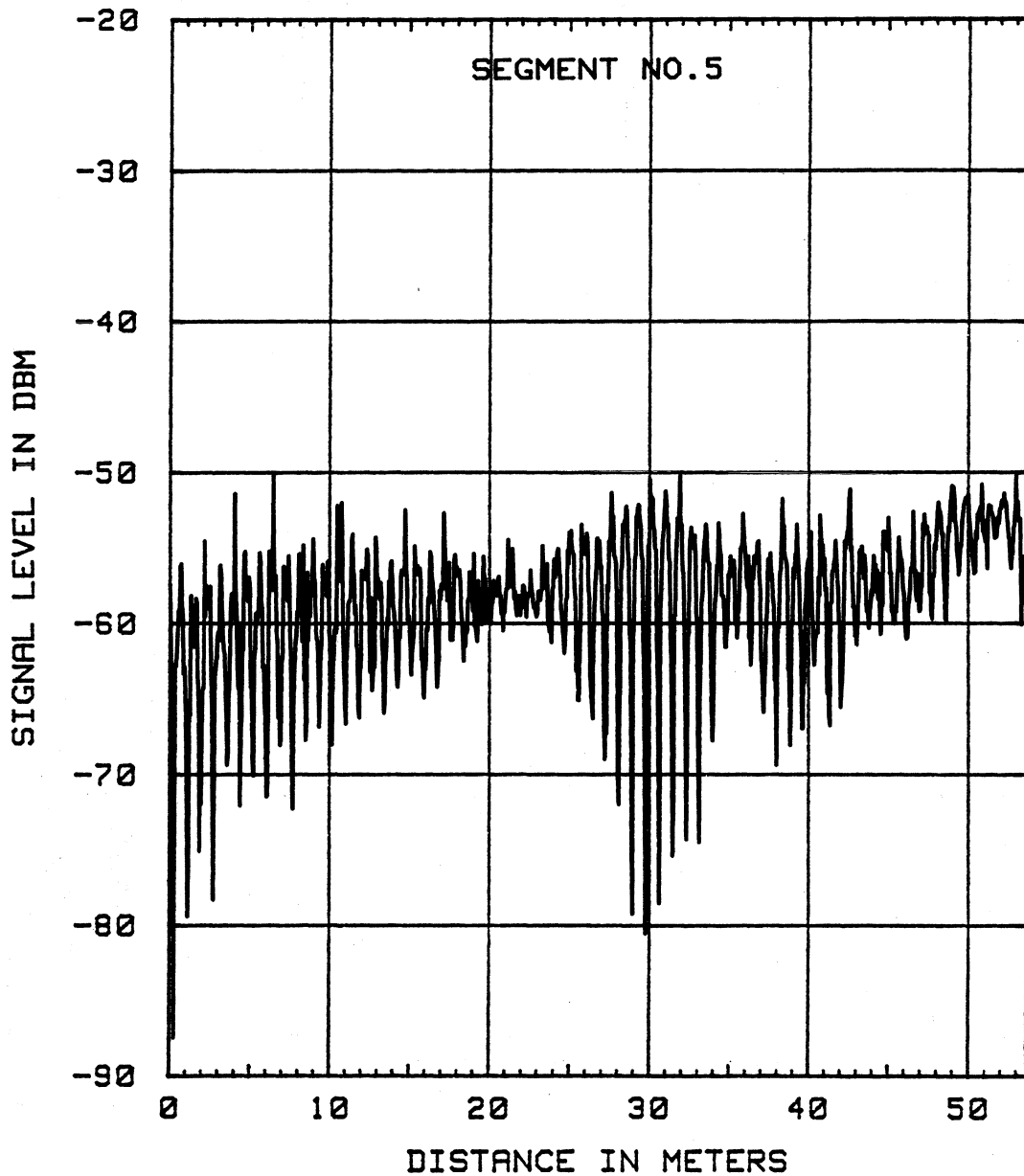


Figure 22. 14 August '79 data for segment number 5, Channel 9 (KBTU) at 187.24 MHz (Video).

6TH AVE., VALLEY HWY., I-70 LOOP. 8/14/79

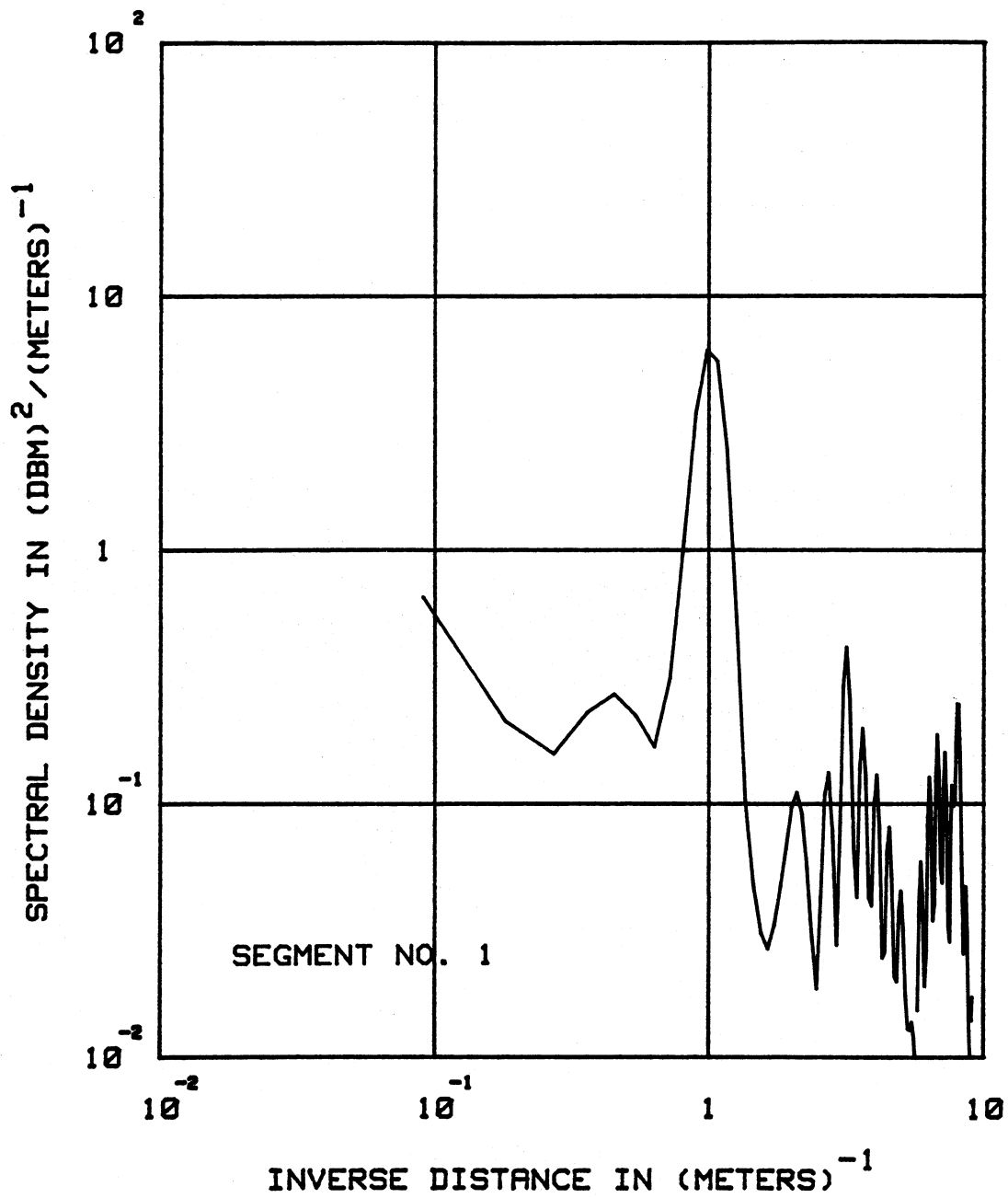


Figure 23. Power spectrum for segment number 1.

6TH AVE., VALLEY HWY., I-70 LOOP. 8/14/79

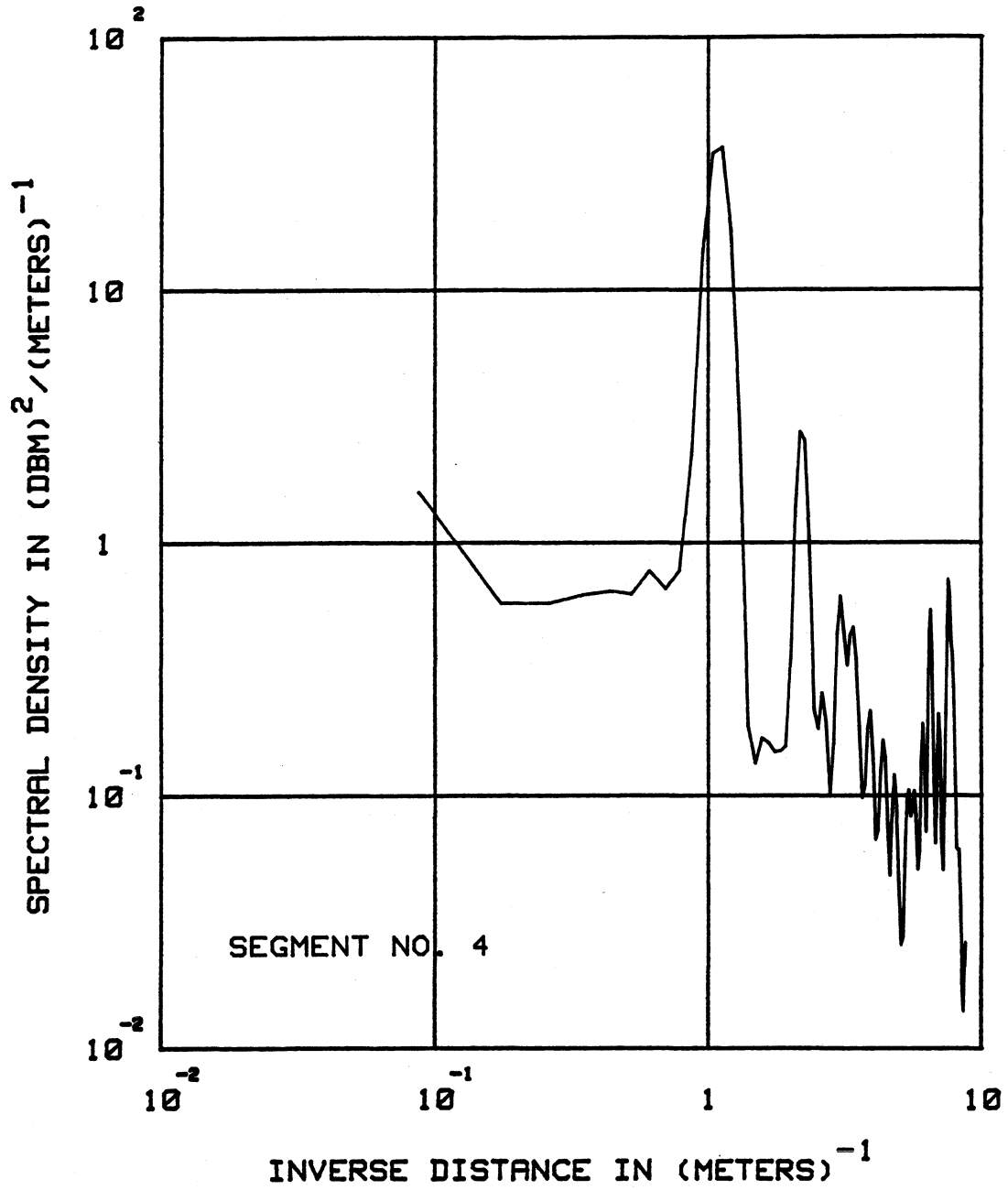


Figure 24. Power spectrum for segment number 4.

6TH AVE., VALLEY HWY., I-70 LOOP. 8/14/79

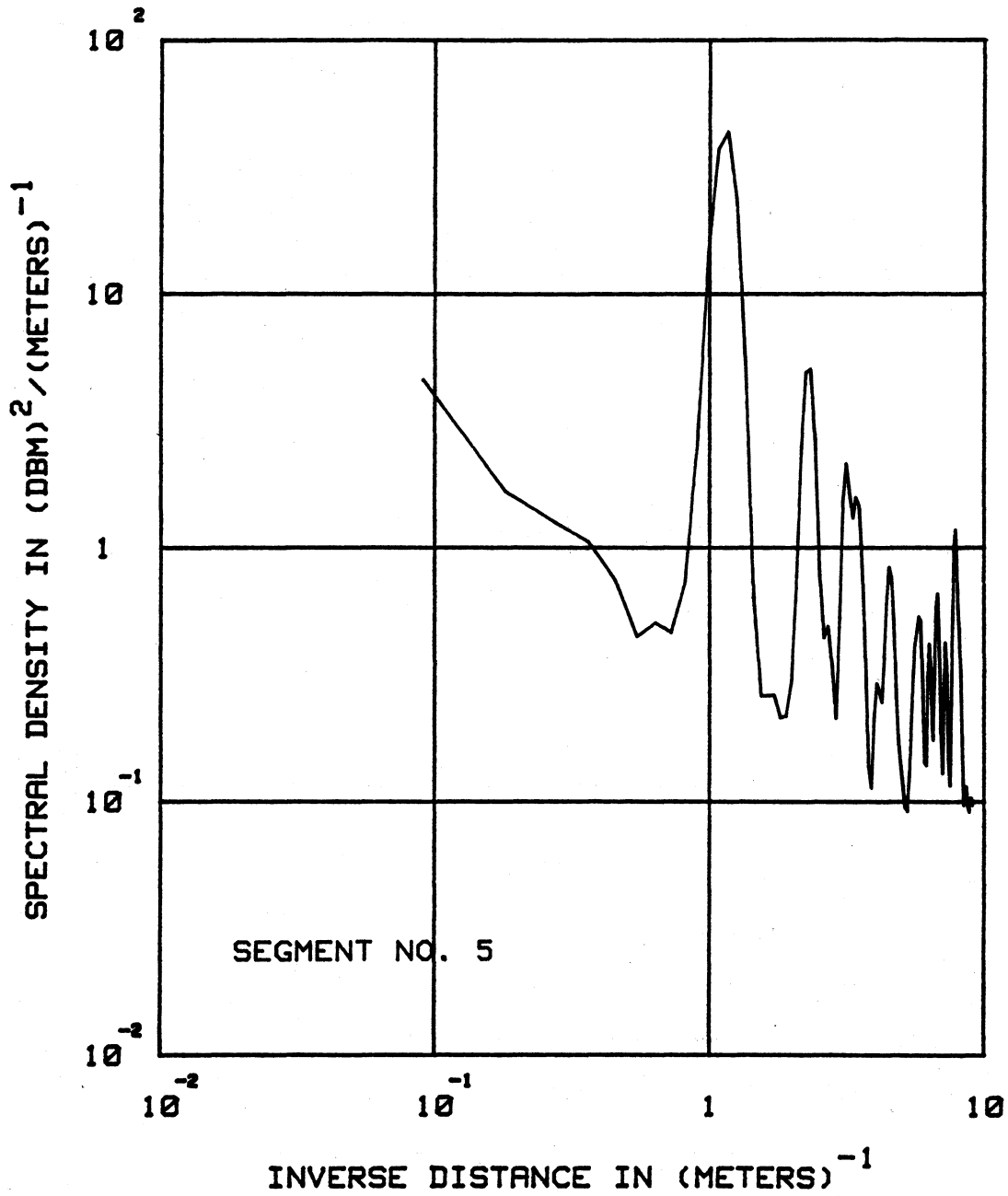


Figure 25. Power spectrum for segment number 5.

$$p(R; \sigma, n) = \frac{n}{\sigma} \left(\frac{R}{\sigma}\right)^{n-1} \exp \left[- \left(\frac{R}{\sigma}\right)^n \right] \quad (3)$$

where σ is the scale parameter, R is the signal envelope, and the Weibull CDF is found directly as

$$\begin{aligned} P(R; \sigma, n) &= \int_R^{\infty} p(R; \sigma, n) dR \\ &= \exp \left[- \left(\frac{R}{\sigma}\right)^n \right] . \end{aligned} \quad (4)$$

The exponent, n , can be obtained from the slope of the straight line approximation of the CDF where the slope (S) is related to the exponent by $S = 2/n$. Thus, for the four distributions (segments 1, 4, 5, and 24) shown in Figure 26, the values of n are 5.9, 3.2, 2.4, and 2.0, respectively. It is easily seen that when the exponent $n = 2$, equation (4) becomes the Rayleigh distribution function of equation (2).

The physical interpretation of the variation in cumulative distribution function (CDF) is that the deviation in slope from that of a Rayleigh distribution give a measurement of the degree of change of the composite received signal envelope from a random multipath characteristic; i.e., as the absolute values of slope decrease below 1 (Rayleigh value), the more nearly the random component of the signal envelope is reduced. Indeed, even a casual inspection of the data shows that, when a standing wave pattern is observed in the data time plot (Figures 20 and 22), the CDF plot for this data shows a slope much less than 1.

4. DISCUSSION AND RECOMMENDATIONS

As was stated in the preceding section, the data presented in this report show a spatially nonstationary characteristic. This can be clearly seen from Figure 27, where the standard deviation of each data segment is plotted as a function of position (segment) on the 30 mi course through Denver. The entire 52 segments were recorded in a time period of 55 minutes. It is thus clear that the standard deviation is not a constant, but varies with time in some manner $\sigma(t)$, which expresses the fact that either the number or the magnitude of the component waves is varying as the measurement van changes position in the urban environment. Because of this nonstationary (time dependent) quality, the statistical analysis is difficult to interpret. Nevertheless, attempts have been made to normalize mobile-radio data to a "local" mean (Clarke, 1968), thereby retaining the assumption that the field is completely scattered and thus forcing the expected distribution of the signal envelope to be Rayleigh. The plot of the means of the data segments in Figure 28 shows the difficulty in trying to define a "local" mean since the mean varies by more than 20 dB.

SEGMENTS 1, 4, 5, & 24 of 14 AUGUST 1979
 CUMULATIVE PROBABILITY DISTRIBUTIONS FOR 187.24 MHz (VIDEO)

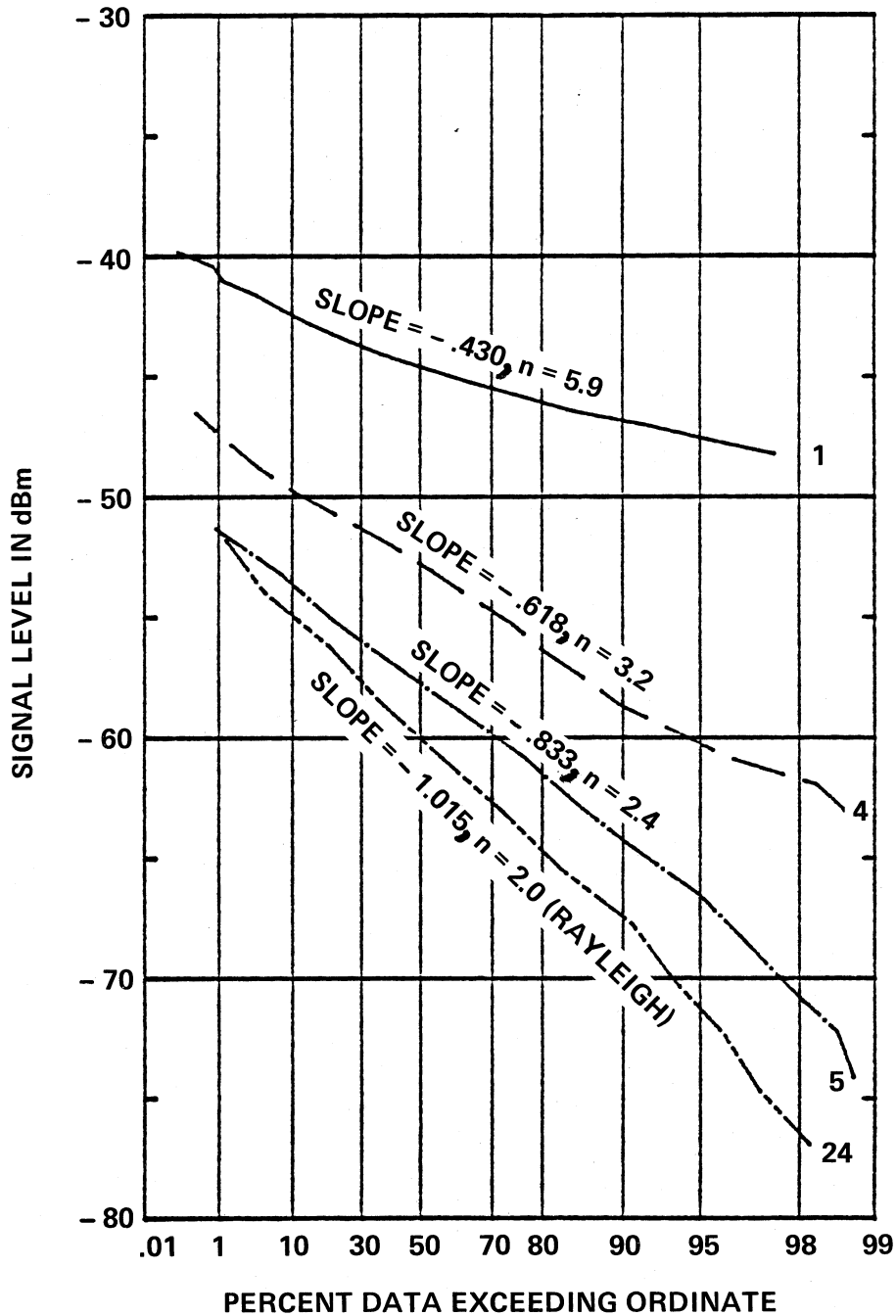


Figure 26. Composite plot of CDF for segments 1, 4, 5, and 24 showing the deviation from a Rayleigh distribution that can occur in the urban environment.

6TH AVE., VALLEY HWY., I-70 LOOP. 8/14/79

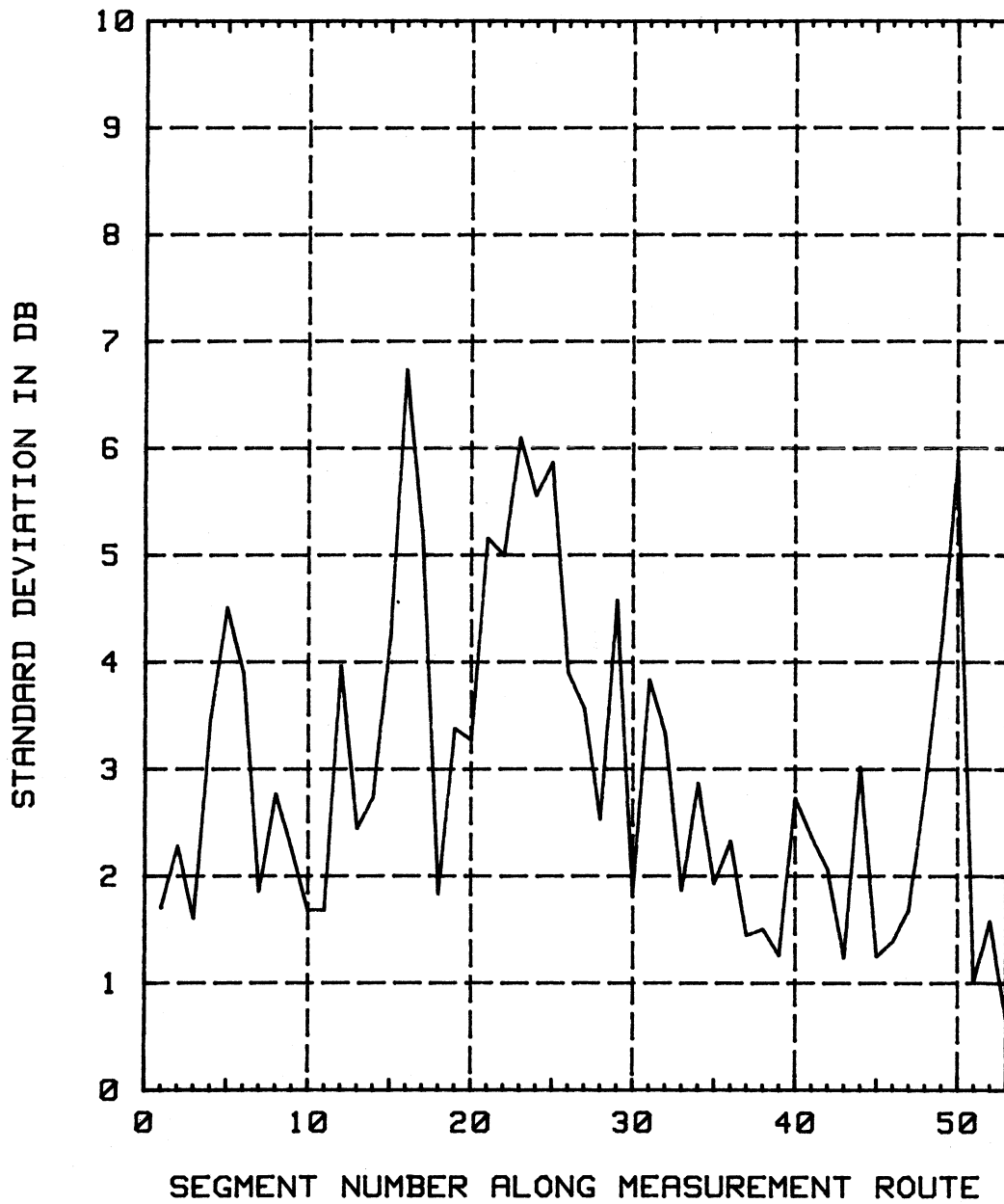


Figure 27. Standard deviation of the data segments on the 14 August 1979 6th Avenue, Valley Highway, I-70 loop.

6TH AVE., VALLEY HWY., I-70 LOOP. 8/14/79

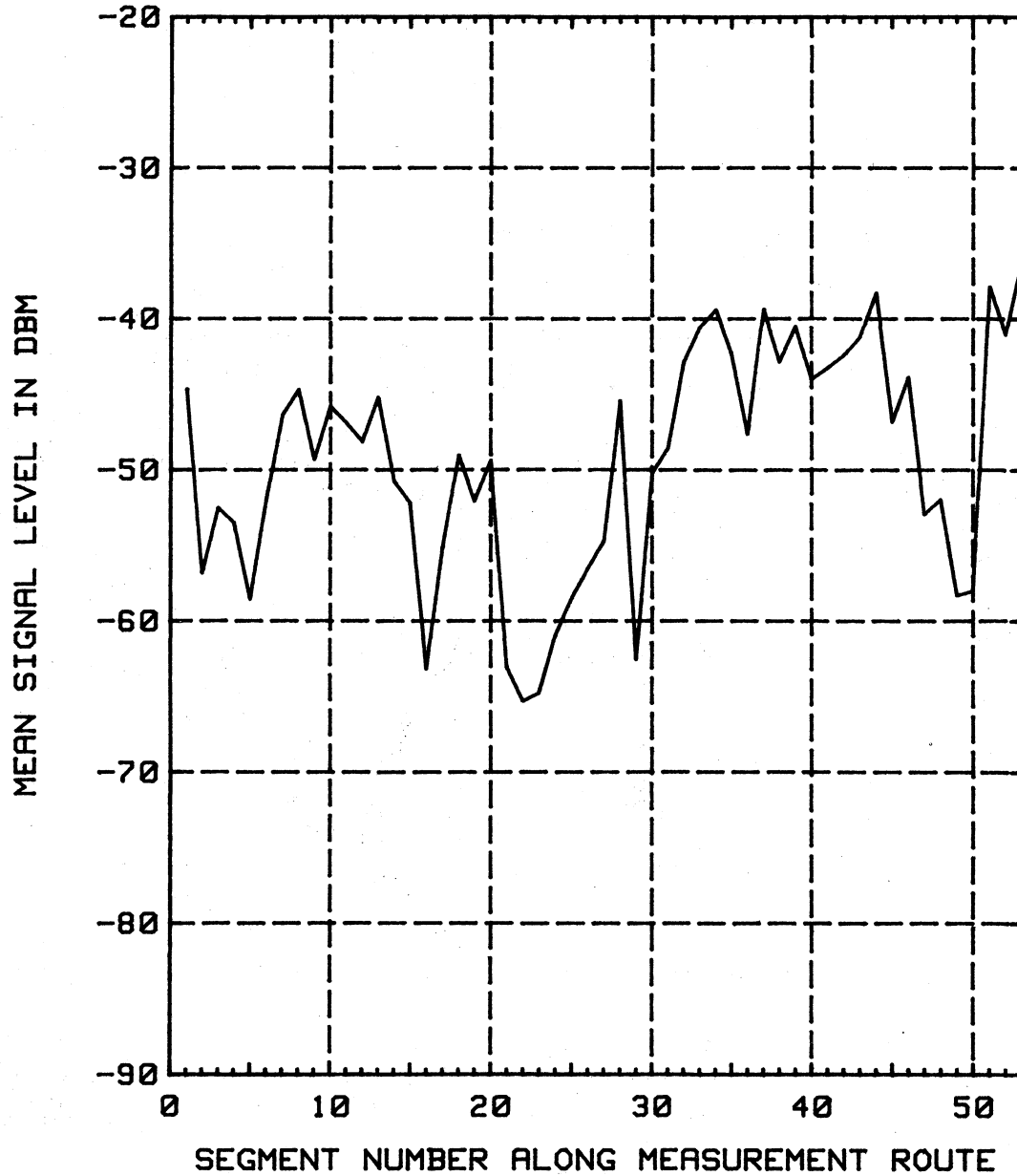


Figure 28. Mean value of the signal envelope for each data segment of 14 August 1979.

The most general conclusion that can be reached from the analysis presented in this paper is that the approach of normalizing the data by calculating a power density spectrum as a function of an inverse distance (wave number) gives a means of comparing data, taken at different times on different days and at different vehicle velocities, in such a way as to at least separate the stationary properties from the nonstationary effects. As would be expected the probability density distribution is only "Rayleigh" when there are no strong specularly reflected waves (which would appear to occur only for special cases in the urban environment) and the main line-of-sight beam from the transmitting antenna is obscured from the receiving antenna on the moving vehicle by large buildings, terrain, etc. Furthermore, we have shown that the actual cumulative distribution function for mobile reception of VHF can be characterized by an exponential probability distribution (Weibull model) that gives the degree of deviation of the received signal envelope from a random (Rayleigh) multipath effect.

In the future it is hoped to extend these measurements into the UHF band and carry out the analysis techniques, that were developed at VHF, at the higher frequencies. It would also be desirable to measure the VHF/UHF signals in the Denver metropolitan area during different seasons of the year under various meteorological conditions to give a larger data base for looking at the time dependent aspects of the data that have only been analyzed to a limited degree in this paper.

5. REFERENCES

- Blackman, R. B., and J. W. Tukey (1958), The Measurement of Power Spectra from the Point of View of Communication Engineering, (Dover Publications Inc., New York, New York).
- Clarke, R. H. (1968), A statistical theory of mobile radio reception, Bell System Tech. J. 47, pp. 957-1000.
- Dougherty, H. T. (1967), Microwave fading with airborne terminals, ESSA Tech. Rept. IER 58ITSA55.
- Harris, F. J. (1978), On the use of windows for harmonic analysis with the discrete Fourier transform, Proc. IEEE 66, No. 1, January.
- Jakes, W. C. (1974), Microwave Mobile Communications, Chapter 1, (John Wiley and Sons).
- Norton, K. A., L. E. Vogler, W. V. Mansfield, and P. J. Short (1955), The probability distribution of the amplitude of a constant vector plus a Rayleigh-distributed vector, Proc. IRE 43, No. 10, pp. 1354-1361.

Ossanna, J. F., Jr. (1964), A model for mobile radio fading due to building reflections: Theoretical and experimental fading waveform power spectra, Bell System Tech. J. 43, pp. 2935-2971.

Weibull, W. (1951), A statistical distribution of wide applicability, J. App. Mech., Trans. A.S.M.E. 73.

APPENDIX. THE POWER SPECTRUM COMPUTATION

The power spectrum is equal to the Fourier transform of the autocovariance function of the input time series. The computing method used here consists of: (1) preliminary (and optional) smoothing, decimation, and prewhitening of the input data; (2) computation of the autocovariance function; (3) modification of the autocovariance function by use of the "Parzen lag window"; (4) computation of the Fourier transform of the modified autocovariance function to produce a "raw" power spectrum; and (5) correction of the "raw" spectrum to take into account the preliminary processing of the input data.

Preliminary Data Processing

Smoothing and decimation. One of the first decisions to be made in a power spectrum analysis is the frequency range over which the spectrum is to be estimated (Blackman and Tukey, 1958, page 44-45). If the original time series consists of data read at intervals of Δt seconds, then the highest frequency for which a spectral density can be computed is $1/(2\Delta t)$, where $m\Delta t$ is the maximum lag to which the autocovariance function is computed. The value of m is usually chosen on the bases of stability of the spectral estimates (inversely proportional to m) and time and cost of computation (almost directly proportional to m). Hence, increasing m in order to extend the spectrum computation to lower frequencies is often not practical. Instead, Δt can be increased by a factor X by using averages of non-overlapping groups of X points as input to the computation.

The principal hazard inherent in this procedure is aliasing, (Blackman and Tukey, 1958, page 31-33) or the erroneous addition to the spectral densities within the computed frequency range of variance contributions that actually come from higher frequencies. The frequency $1/(2\Delta t)$ is called the Nyquist or folding frequency. Any variance contributions from frequencies above $1/(2\Delta t)$ are "folded" onto the computed spectrum; the spectral densities from $1/(2\Delta t)$ to $1/\Delta t$ are added to those from $1/(2\Delta t)$ to 0, respectively; those from $1/\Delta t$ to $3/2\Delta t$ are added to those from 0 to $1/(2\Delta t)$, respectively, and so on.

Fortunately, aliasing can be reduced by filtering out frequencies above $1/2\Delta t$ before sampling the data or, to a lesser degree, by averaging the data after sampling, as described above. Furthermore, aliasing is less important if the spectrum decreases rapidly with increasing frequency, as is often the case in radio propagation data. However, it cannot be entirely eradicated, and one should be prepared to view with some suspicion the spectral densities near the folding frequency, where aliasing is usually most troublesome.

Prewhitening. Most of the time series used as input to the power spectrum computation (Blackman and Tukey, 1958, page 39-42) can be expected to contain large long-term trends; i.e., fluctuations with periods long compared to the sample length, and with amplitudes large enough to make a significant contribution to the sample variance. Although the variance contribution is actually made at frequencies below the lowest computed spectral frequency, the computed spectral estimates will be contaminated by the trend variance unless the trends are removed beforehand. Any procedure used to remove trends is commonly referred to as "prewhitening" since, by reducing the large low-frequency components present in the raw data, the computed spectrum more closely resembles the spectrum of white noise. Subsequently, of course, the computed spectrum must be corrected for the effects of prewhitening, so that the final result accurately indicates the variance contribution from a given frequency region.

The prewhitening procedure used in this case consists of simply of using first differences of the original data as input to the spectrum computation. That is, if y_1', y_2', \dots, y_n' is the original time series, y_i' is replaced by

$$y_i = 0.5 (y_i' - y_{i+1}') \quad (A1)$$

This operation is equivalent to passing the original data through a high-pass filter with a frequency response given by

$$P(f) = (\sin (\pi f \Delta t))^2, \quad (A2)$$

where Δt is the sampling period; i.e., the time interval between adjacent elements of the time series. Subsequently, to obtain an estimate of the power spectrum of the original data, the computed spectrum must be multiplied by $(P(f))^{-1}$.

In order to normalize the Power spectrum for data taken at different times and at different vehicle speeds, we introduce a change of variable. The sampling period (data spacing Δt in seconds) is converted to a distance spacing Δd in meters: $\Delta d = v \Delta t$, where v = vehicle speed in meters/sec. Thus in the following we will outline a method for computing a "wave number" spectrum rather than a frequency spectrum.

Autocovariance Function

The autocovariance function is given by

$$A'(k) = \frac{1}{n-k} \left(\sum_{i=1}^{n-k} X_i X_{i+k} - \frac{1}{n-k} \sum_{i=1}^{n-k} X_i \sum_{i=1}^{n-k} X_{i+k} \right) \quad (A3)$$

where n is the number of original data points and $k = 0, 1, \dots, m$.

As was mentioned previously, m is also the number of points on the resulting power spectrum graph. Along with Δd , m also determines the minimum non-zero interval for which the spectral density is computed, $\frac{1}{2m\Delta d}$. The maximum interval is $\frac{1}{2\Delta d}$, so that m is the ratio of maximum to minimum interval. For the sake of convenience we will call this interval the "wave number".

The Parzen Lag Window

Because of practical limits which must be placed on the number of data points, n , and the number of lags, m , that can be used in any given computation, a process called "windowing" must be applied either to the autocovariance function (using a "lag window") or to the power spectrum (using a "spectral window") in order to obtain statistically manageable results (Blackman and Tukey, 1958, page 11-17, Harris, 1978).

The lag window used here is called the Parzen window, defined as

$$L(k) = \begin{cases} 1 - 6 \left(\frac{k}{m}\right)^2 + 6 \left|\frac{k}{m}\right|^3, & \left|\frac{k}{m}\right| < \frac{1}{2} \\ 2 \left(1 - \left|\frac{k}{m}\right|\right)^3, & \frac{1}{2} \leq \left|\frac{k}{m}\right| \leq 1 \end{cases} \quad (A4)$$

The modified or "windowed" autocovariance function is given by

$$A(k) = L(k) A'(k) \quad (A5)$$

The Power Spectrum

The power spectrum of the prewhitened data, $W'(u)$, is the Fourier transform of the windowed autocovariance function, $A(k)$. It is given by

$$W'(u_h = \frac{h}{2m\Delta d}) = 4\Delta d \left(\frac{1}{2} \left(A(0) + (-1)^h A(m) \right) + \sum_{k=1}^{m-1} A(k) \cos\left(\frac{\pi kh}{m}\right) \right), \quad (A6)$$

$h = 0, 1, 2, \dots, m;$

$W'(u_h)$ has the dimensions of variance per unit wave number. If Δu_h is the wave number associated with the spectral density $W'(u_h)$, then the total variance of the prewhitened data is given by

$$\text{total variance} = \sum_{h=0}^m W'(u_h) \Delta u_h \quad (A7)$$

The interval Δu_h for $h=1$ to $m-1$ is equal to $\frac{1}{2m\Delta d}$, while for $h=0$ and m , the interval is $\frac{1}{4m\Delta d}$.

In the section on prewhitening, it was mentioned that if the input data has been prewhitened (as is usually the case), the final step in the power spectrum computation is to compensate for the effects of prewhitening by multiplying the spectrum by the inverse of the prewhitening filter response; i.e.,

$$W(u_h) = W'(u_h) (\sin(\pi u_h \Delta d))^{-2}. \quad (A8)$$

Since the correction is infinite at $u = 0$, $W(0)$ is not computed when the prewhitening scheme is employed.

The "wave number" spectrum we have calculated here is not a "power spectrum" in the strictest sense of the word, i.e., if we consider $X(t)$ as the current through a pure resistance of one ohm, then the average power dissipated in the resistance will be directly proportional to the variance of $X(t)$. This special case is the origin of the adjective "power". The use of the technique, however, is not restricted to power applications, and has been used, for example, in the analysis of turbulence spectra in meteorology.

We have been able to use this technique for calculating a spectral density to normalize the mobile VHF measurements made in the Denver, Colorado metropolitan area at different times and at various vehicle velocities. The effect of this "normalization" is to sort out the peaks (standing wave patterns) in the spectra which are characteristic of the fixed topographical scattering surfaces that appear to be always present along a measurement route, from those that change from one measurement time to another. Furthermore, these fixed surfaces appear to be dominant scatterers. There may be other fixed scattering surfaces making sufficiently small contributions to the "power" spectrum that they cannot be distinguished in the spectrum. Although it is difficult to make an exact physical justification for the mathematical procedure we have used here, the heuristic approach to defining and using a "wave number" spectrum leads to some interesting results. The major one being that certain peaks in the spectra are present for data taken at different times and at vehicle speeds varying from 10 to 40 mph as shown in Figures 19, 23, 24, and 25 of the main text.

BIBLIOGRAPHIC DATA SHEET

1. PUBLICATION NO. NTIA Report 81-60		2. Gov't Accession No.	3. Recipient's Accession No.
4. TITLE AND SUBTITLE Some Mobile VHF Measurements in an Urban Environment		5. Publication Date January 1981	
		6. Performing Organization Code	
7. AUTHOR(S) C. J. Chilton, H. B. Janes, R. A. McLean, and D. Smith		9. Project/Task/Work Unit No. 910 8102	
8. PERFORMING ORGANIZATION NAME AND ADDRESS National Telecommunications & Information Admin. Institute for Telecommunication Sciences 1-3449 325 Broadway Boulder, CO 80303		10. Contract/Grant No.	
11. Sponsoring Organization Name and Address U.S. Dept. of Commerce National Telecommunications & Information Admin. 1325 G. Street, NW Washington, DC 20005		12. Type of Report and Period Covered	
		13.	
14. SUPPLEMENTARY NOTES			
15. ABSTRACT (A 200-word or less factual summary of most significant information. If document includes a significant bibliography or literature survey, mention it here.) This paper presents the results of mobile measurements of VHF signals in the Denver, Colorado, urban environment. The signals monitored were those received from the TV transmissions of KBTW (Channel 9), KMGH (Channel 7), KOA (Channel 4), and KWGN (Channel 2) from transmitting antennas located on top of Lookout Mountain. The statistical analysis of the data implies that the signal fading mechanism does not always have Rayleigh probability density distribution, and could possibly be better described by an exponential Weibull distribution. In addition, a new analysis technique was developed to normalize the data by calculating a power density spectrum as a function of an inverse distance (wave number) which gives a means of comparing data taken at different times on different days and at different vehicle velocities in such a way as to make it possible to separate the position dependent effects from the time dependent properties.			
16. Key Words (Alphabetical order, separated by semicolons) Key Words: mobile radio communication; statistical analysis; VHF; VHF radio propagation			
17. AVAILABILITY STATEMENT <input checked="" type="checkbox"/> UNLIMITED. <input type="checkbox"/> FOR OFFICIAL DISTRIBUTION.		18. Security Class. (This report) Unclassified	20. Number of pages 42
		19. Security Class. (This page) Unclassified	21. Price:

